

SUPPORTING INFORMATION

Maghemite decorated with ultra-small palladium nanoparticles (γ -Fe₂O₃-Pd): applications in Heck-Mizoroki olefination, Suzuki reaction and allylic oxidation of alkenes

Anuj K. Rathi,^a Manoj B. Gawande,^{a*} Jiri Pechousek,^a Jiri Tucek,^a Claudia Aparicio,^a Martin Petr,^a Ondrej Tomanec,^a Radka Krikavova,^b Zdenek Travnicek,^b Rajender S. Varma,^c and Radek Zboril^{a*}

^aRegional Centre of Advanced Technologies and Materials, Faculty of Science, Department of Physical Chemistry, Palacky University, Šlechtitelů 27, 783 71, Olomouc, Czech Republic.

^bRegional Centre of Advanced Technologies and Materials, Faculty of Science, Department of Inorganic Chemistry, Palacky University, Šlechtitelů 27, 783 71, Olomouc, Czech Republic.

^cSustainable Technology Division, National Risk Management Research Laboratory, US Environmental Protection Agency, 26 West Martin Luther King Drive, MS 443, Cincinnati, Ohio, 45268, USA.

Contents

General information	2
Characterization techniques	2-3
Experimental analysis	4
TEM and HRTEM images showing size and morphology of reused catalyst	4-5
Comparison with earlier heterogeneous Catalyst used	5-9
Reusability study	9
XPS spectrum of reused catalyst	9
Characterization data of compounds	10-16
NMR spectra of compounds	17-35
References	36

General information. All commercial reagents were used as received unless otherwise mentioned. For analytical and preparative thin-layer chromatography, Merck, 0.2 mm and 0.5 mm Kieselgel GF 254 pre-coated were used, respectively. The spots were visualized with iodine, and UV light.

Characterization techniques

X-ray powder diffraction (XRD) patterns for maghemite and maghemite-Pd samples were recorded at room temperature using a X’Pert PRO MPD diffractometer (PANalytical) in Bragg–Brentano geometry with iron-filtered, Co-K α radiation (40 kV, 30 mA, $\lambda = 0.1789$ nm) equipped with an X’Celerator detector and programmable divergence and diffracted beam antiscatter-slits. The angular range of measurement was set as $2\theta = 10\text{--}105^\circ$, with a step size of 0.017° . The identification of the crystalline phases in the experimental XRD pattern was obtained using the X’Pert High Score Plus software that includes a PDF-4+ and ICSD databases. Scanning Electron Microscope (SEM) was performed on Hitachi SU6600 with accelerating voltage 15 kV. Energy Dispersive Spectrometry (EDS) was acquired in SEM by Thermo Noran System 7 with Si(Li) Detector. Accelerating voltage was 15 kV and acquisition time was 300 s.

Microscopic images were obtained by HRTEM TITAN 60-300 with X-FEG type emission gun, operating at 80 kV. This microscope is equipped with Cs image corrector and a STEM high-angle annular dark-field detector (HAADF). The point resolution is 0.06 nm in TEM mode. The elemental mappings were obtained by STEM-Energy Dispersive X-ray Spectroscopy (EDS) with acquisition time 20 min. For HRTEM analysis, the powder samples were dispersed in ethanol and 5 min ultrasonicated. One drop of this solution was placed on a copper grid with holey carbon film. The sample was dried at room temperature.

XPS surface investigation has been performed on the PHI 5000 VersaProbe II XPS system (Physical Electronics) with monochromatic Al-K α source (15 kV, 50 W) and photon energy

of 1486.7 eV was employed. Dual beam charge compensation was used for all measurements. All the spectra were measured in the vacuum of 1.3×10^{-7} Pa and at the room temperature of 21 °C. The analyzed area on each sample was spot of 200 µm in diameter. The survey spectra was measured with pass energy of 187.850 eV and electronvolt step of 0.8 eV while for the high resolution spectra was used pass energy of 23.500 eV and electronvolt step of 0.2 eV. The spectra were evaluated with the MultiPak (Ulvac - PHI, Inc.) software. All binding energy (BE) values were referenced to the carbon peak C1s at 284.80 eV.

The transmission ^{57}Fe Mössbauer spectra were recorded on homemade Mössbauer spectrometer operating at a constant acceleration mode and equipped with 50 mCi $^{57}\text{Co}(\text{Rh})$ source. For low-temperature (5 K) and in-field (5 T) measurements, the sample was placed inside the chamber of the Spectromagcryomagnetic system (Oxford Instruments); with the Mössbauer spectrometer attached to the system, the setup works in a parallel geometry when the external magnetic field is applied in a parallel direction with respect to the propagation of γ -rays. For fitting the Mössbauer spectra, the MossWinn software program was used. The isomer shift values are referred to α -Fe at room temperature. NMR spectra were measured in DMSO- d_6 on a JNM-ECA600II NMR spectrometer (JEOL, Japan) at 298 K. Tetramethylsilane (TMS) was used as the internal reference standard for ^1H and ^{13}C NMR experiments. The conversion and selectivity of the reactions were analyzed by GC employing chromatograph Agilent 6820 (Agilent, United States), equipped with flame ionisation detector (FID) and chromatographic column DB5 (30x0.250x0.25). Following experimental parameters were applied: initial temperature 100 °C, increased to 250 °C with a rate of 10 °C/min.

Experimental analysis

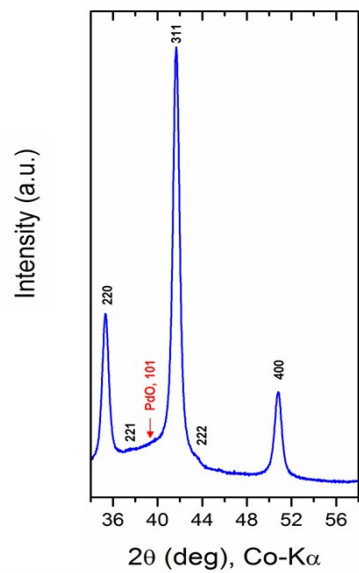
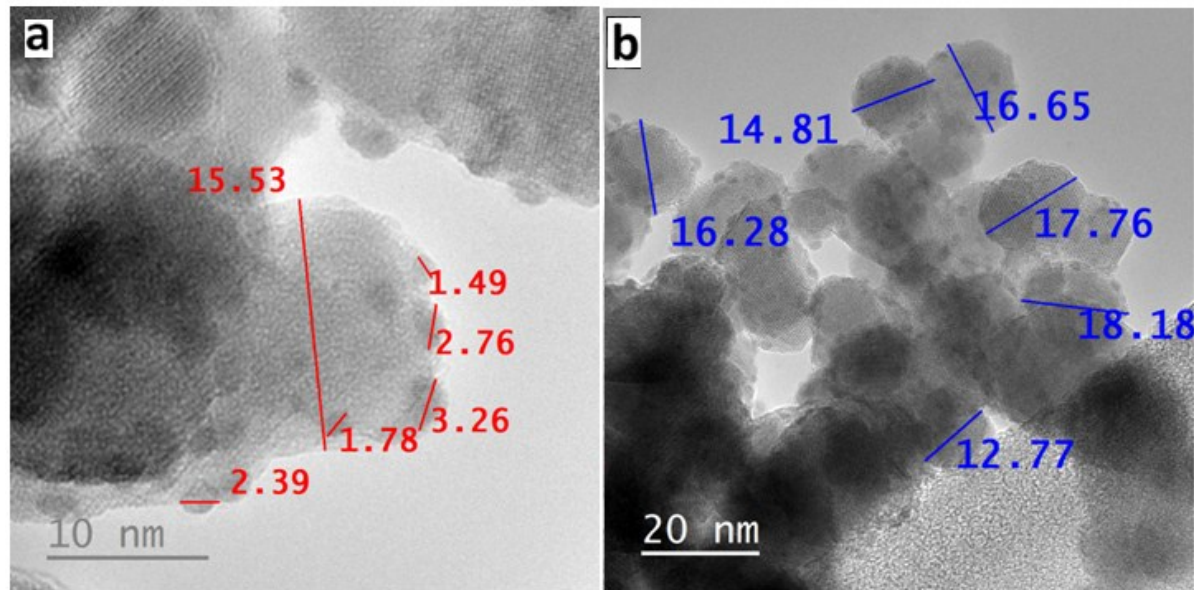


Fig. S1. Miller indices, corresponding to maghemite and PdO are shown in black and red numbers, respectively.



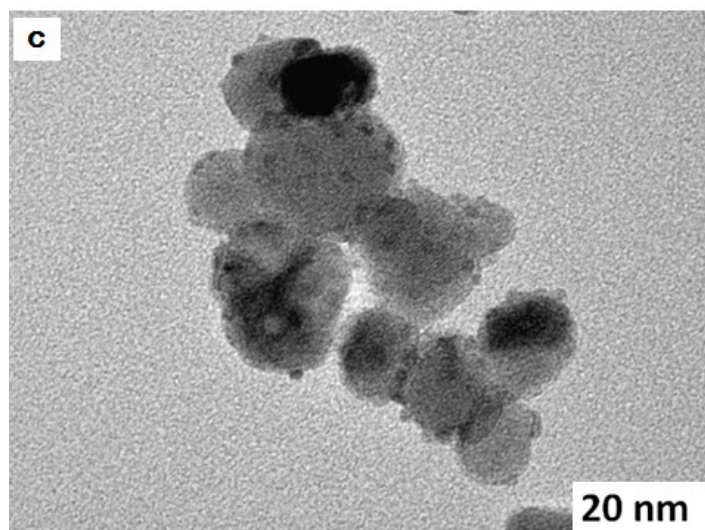


Fig. S2. (a-b) HRTEM images of maghemite-Pd showing ultrasmall Pd nanoparticles (<5 nm) covering globular (maghemite nanoparticles (ca. 10-20) nm. (c) TEM image of maghemite-Pd nanoparticles in Suzuki reaction after four cycles.

Table S1. Comparison of selected heterogeneous catalysts used for Suzuki reaction.

Entry	Catalyst	Conditions	Yield (%) ^a	Ref.
1	Pd(0)/C	TBAB, 2 M Na ₂ CO ₃ , DME, 80 °C, O/N	21-95%	1
2	Pd/MgLa mixed oxide	80 °C, Ethanol, K ₂ CO ₃ , 1-6h	37-98	2
3	Pd ⁺² -sepiolite	100-130 °C, K ₂ CO ₃ , DMF, 20-24h	23-94 ^b	3
4	Pd HAP-1 (2 X 10 ⁻³)	120 °C, K ₂ CO ₃ , o-Xylene, 4-24 h	80-98 ^b	4
5	Pd (II)-SBA-16	Pd (II)-SBA-16, K ₂ CO ₃ , 80 °C, EtOH : H ₂ O, 2.5-12 h	28-99	5
6	PANI-Pd	95 °C, K ₂ CO ₃ , Dioxane: H ₂ O, 4h	75-95	6
7	SBA-15-XH-Pd	100 °C, DMF: H ₂ O, NaOAc, 15h	67-98	7
8	Maghemite-Pd	100°C, K ₂ CO ₃ , DMF: H ₂ O, 2h	60-95	Present work

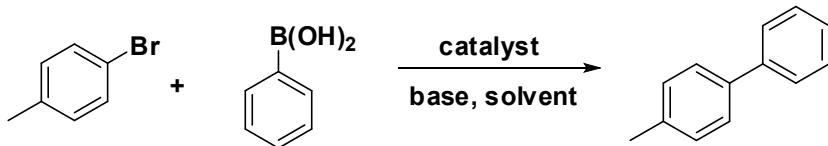
^a Isolated yield, ^bGC yield

Table S2. Comparison of selected heterogeneous catalyst used for Heck reaction.

Entry	Catalyst	Conditions	Yield ^a (%)	Ref.
1	SBA-15-XH-Pd	100 °C, DMF, K ₂ CO ₃ , 15h	93-97	7
2	Pd-MCM-41	150 °C, Na ₂ CO ₃ , Bu ₄ NCl, NMP, 3-22h	54-100 ^c	8
3	PANI-Pd	140 °C, K ₂ CO ₃ , DMA, 40 h	41-98	6
4	{[Pd(NH ₃) ₄]/NaY}	140 °C, NaOAc, NMP, 6-24 h	23-79	9
5	C-(KTB-Pd)	120 °C, K ₃ PO ₄ ·3H ₂ O, DMF, 2-12h	72-99	10
6	Maghemite-Pd	110°C, K ₂ CO ₃ , DMF, 1h	60-95	Present work

^a Isolated yield, ^bGC yield, ^cConversion

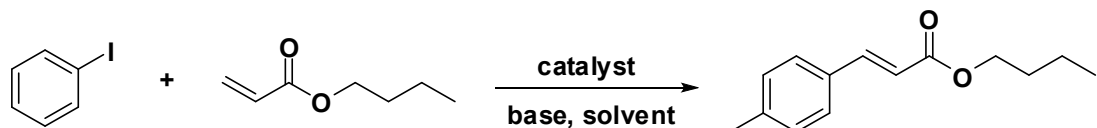
Table S3. TOF comparison of various supported Pd catalysts for the reaction of 1-bromo-4-methylbenzene with phenyl boronic acid.



Entry	Pd Catalyst (mol %)	Conditions	TOF (h ⁻¹)	Ref.
1	Fe ₃ O ₄ -Bpy-Pd(OAc) ₂	K ₂ CO ₃ , toluene, 12h, 80 °C	4	11
2	Pd- Fe ₃ O ₄ @C	K ₂ CO ₃ , EtOH, 2h, 60 °C	37	12
3	Pd-Fe ₃ O ₄ heterodimer NCs	K ₃ PO ₄ , 1,4-dioxane, 24h, reflux	29	13
4	Pd-SBA-16	K ₂ CO ₃ , EtOH: H ₂ O, 8h, 80 °C	10	14
5	SBA-15-SH-Pd	K ₂ CO ₃ , DMF: H ₂ O, 15h	54	15
6	Maghemite-Pd	100°C, K ₂ CO ₃ , DMF: H ₂ O, 2h	43	Present work

$$TOF \left(h^{-1} \right) = \frac{Yield}{\frac{100}{Time \left(h \right)}} X \frac{mmol \text{ of reactant}}{mmol \text{ of Pd}}$$

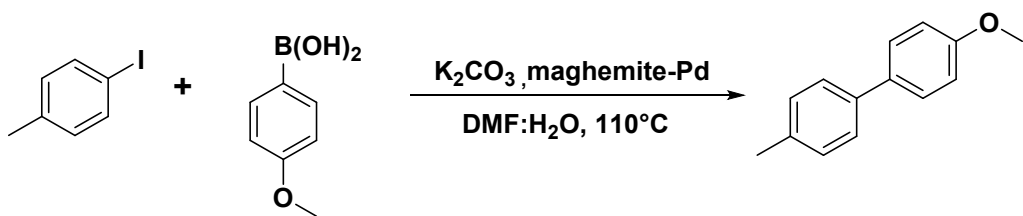
Table S4. TOF comparison of various supported Pd catalysts for the reaction of iodobenzene with butyl acrylate.



Entry	Catalyst	Conditions	TOF(h^{-1})	Ref.
1	$\text{Fe}_3\text{O}_4\text{-NH}_2\text{-Pd}$	K_2CO_3 , NMP, 130 °C, 10h	10	16
2	Pd-PVP@laponite	Et_3N , 100 °C, 4h	70 ^a	17
3	MNP@NHC-Pd	NaHCO_3 , DMF, reflux, 3h	2	18
4	Maghemite-Pd	100°C, K_2CO_3 , DMF: H_2O , 2h	31	Present work

^a GC yield,

Table S5. Catalyst reusability study.^a



Entry	1 st	2 nd	3 rd	4 th
Conversion (%) ^b	>99	>99	>98	>97
Isolated yield (%) ^c	>94	>94	>93	>92

^aReaction conditions: 1-iodo-4-methylbenzene (0.5 mmol), K_2CO_3 (1 mmol), 4-methoxyphenylboronic acid (0.7 mmol), maghemite-Pd (18 mg, 0.010 mmol of Pd), DMF: H₂O (3 mL), 110°C, ^bConversion was measured by GC analysis, ^cIsolated yield.

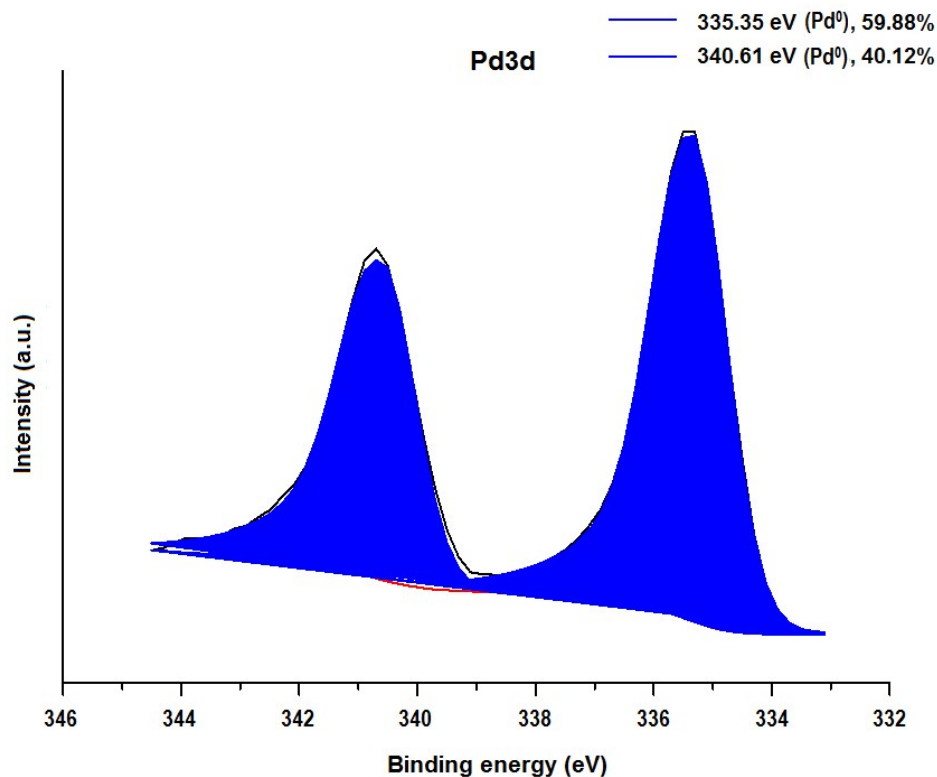
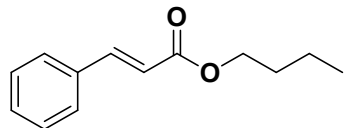


Fig. S3. XPS spectrum of reused maghemite-Pd sample after first cycle. The position of the metallic Pd⁰ is denoted by blue color.

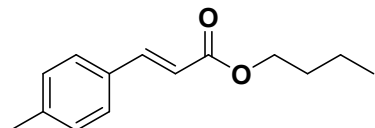
Characterization data of compounds

(E)-Butyl cinnamate (**3a**)¹⁹



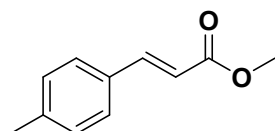
Transparent oil, 94%. ¹H NMR (600 MHz, DMSO-*d*₆): δ= 7.72 (2H, dd, *J*=6.6 Hz, *J*=2.8 Hz), 7.65 (1H, d, *J*=15.9 Hz), 7.42 (3H, m), 6.64 (1H, d, *J*=16.5 Hz), 4.15 (2H, t, *J*=6.6 Hz), 1.62 (2H, qui, *J*= 7.7 Hz), 1.38 (2H, sext, *J*=7.7 Hz), 0.91 (3H, t, *J*=7.4 Hz) ppm. ¹³C NMR (600 MHz, DMSO-*d*₆): δ= 166.28, 144.40, 134.01, 130.45, 128.91, 128.36, 118.12, 63.73, 30.28, 18.67, 13.59 ppm.

(E)-Butyl 3-p-tolylacrylate (**3b**)¹⁹



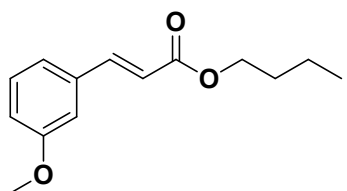
Transparent oil, 95%. ¹H NMR (600 MHz, DMSO-*d*₆): δ= 7.61 (3H, m), 7.23 (2H, d, *J*=8.2 Hz), 6.57 (1H, d, *J*=15.9 Hz), 4.14 (2H, t, *J*=6.6 Hz), 2.32 (3H, s), 1.61(2H, qui, *J*= 7.7 Hz), 1.37 (2H, sext, *J*=7.7 Hz), 0.91 (3H, t, *J*=7.4 Hz) ppm. ¹³C NMR (600 MHz, DMSO-*d*₆): δ= 166.39, 144.38, 140.43, 131.30, 129.52, 128.35, 117.00, 63.63, 30.30, 21.01, 18.67, 13.58 ppm.

(E)-Methyl 3-p-tolylacrylate (**3c**)²⁰



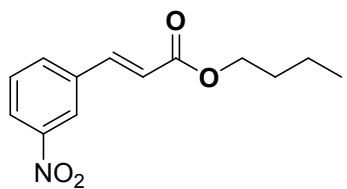
White solid, 93%. ¹H NMR (600 MHz, DMSO-*d*₆): δ= 7.61 (3H, m), 7.23 (2H, d, *J*= 7.7 Hz), 6.57 (1H, d, *J*=15.9 Hz), 3.71 (3H, s), 2.33 (3H, s) ppm. ¹³C NMR (600 MHz, DMSO-*d*₆): δ= 166.79, 144.54, 140.48, 131.27, 129.52, 128.35, 116.67, 51.39, 21.01 ppm.

(E)-Butyl 3-(3-methoxyphenyl)acrylate (3d)¹⁹



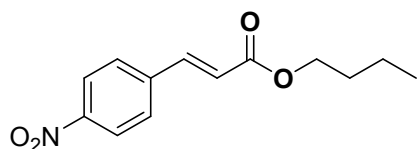
Transparent oil, 95%. ¹H NMR (600 MHz, DMSO-*d*₆): δ= 7.62 (1H, d, *J*=15.9 Hz), 7.32 (2H, m), 7.28 (1H, m), 6.99 (1H, dd, *J*=7.7 Hz, *J*=2.2 Hz), 6.67 (1H, d, *J*=15.9 Hz), 4.15 (2H, t, *J*=6.6 Hz), 3.79 (3H, s), 1.62 (2H, m), 1.38 (2H, sext, *J*=7.7 Hz), 0.91 (3H, t, *J*=7.4 Hz) ppm. ¹³C NMR (600 MHz, DMSO-*d*₆): δ= 166.29, 159.60, 144.36, 135.44, 129.91, 121.00, 118.46, 116.63, 112.86, 63.72, 55.23, 30.28, 18.67, 13.58 ppm.

(E)-Butyl 3-(3-nitrophenyl)acrylate (3e, 3k)²⁰



Light yellow solid, 90% and 88%. ¹H NMR (600 MHz, DMSO-*d*₆): δ= 8.55 (1H, s), 8.22 (2H, m), 7.76 (1H, d, *J*=15.9 Hz), 7.70 (1H, t, *J*=7.8 Hz), 6.85 (1H, d, *J*=16.5 Hz), 4.16 (2H, t, *J*=6.6 Hz), 1.63 (2H, m), 1.38 (2H, sext, *J*=7.5 Hz), 0.91 (3H, t, *J*=7.4 Hz) ppm. ¹³C NMR (600 MHz, DMSO-*d*₆): δ= 165.85, 148.28, 141.96, 135.92, 134.11, 130.32, 124.55, 123.02, 121.13, 63.94, 30.23, 18.64, 13.55 ppm.

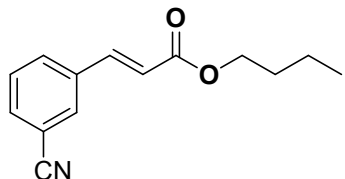
(E)-Butyl 3-(4-nitrophenyl)acrylate (3f, 3i, 3n)²⁰



Yellow solid, 85%, 83%, and 30%. ¹H NMR (600 MHz, DMSO-*d*₆): δ= 8.23 (2H, m), 8.01 (2H, m), 7.75 (1H, d, *J*=16.5 Hz), 6.85 (1H, d, *J*=15.9 Hz), 4.17 (2H, t, *J*=6.6 Hz), 1.63 (2H, qui, *J*=7.7 Hz), 1.38 (2H, sext, *J*=7.7 Hz), 0.92 (3H, t, *J*=7.4 Hz) ppm. ¹³C NMR (600 MHz,

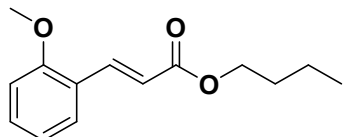
DMSO-*d*₆): δ= 165.73, 148.04, 141.80, 140.47, 129.45, 123.89, 122.43, 64.07, 30.20, 18.63, 13.55 ppm.

(E)-Butyl 3-(3-cyanophenyl)acrylate (3g)²¹



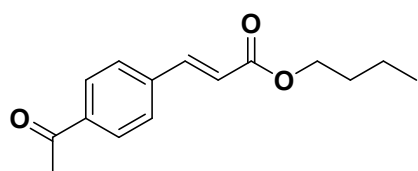
Transparent oil, 62%. ¹H NMR (600 MHz, DMSO-*d*₆): δ= 8.27 (1H, s), 8.07 (1H, d, *J*=7.7 Hz), 7.87 (1H, d, *J*=7.8 Hz), 7.67 (1H, d, *J*=15.9 Hz), 7.62 (1H, t, *J*=7.8 Hz), 6.82 (1H, d, *J*=15.9 Hz), 4.16 (2H, t, *J*=6.6 Hz), 1.63 (2H, m), 1.38 (2H, sext, *J*=7.7 Hz), 0.91 (3H, t, *J*=7.4 Hz) ppm. ¹³C NMR (600 MHz, DMSO-*d*₆): δ= 165.94, 142.10, 135.35, 133.48, 132.79, 131.89, 130.06, 120.66, 118.36, 112.11, 63.93, 30.23, 18.64, 13.56 ppm.

(E)-Butyl 3-(2-methoxyphenyl)acrylate (3h)²²



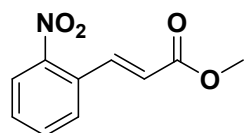
Transparent oil, 82%. ¹H NMR (600 MHz, DMSO-*d*₆): δ= 7.88 (1H, d, *J*=15.9 Hz), 7.71 (1H, dd, *J*=7.7 Hz, *J*=1.1 Hz), 7.42 (1H, t, *J*=7.8 Hz), 7.09 (1H, d, *J*=8.2 Hz), 6.98 (1H, t, *J*=7.4 Hz), 6.60 (1H, d, *J*=15.9 Hz), 4.14 (2H, t, *J*=6.6 Hz), 3.87 (3H, s), 1.62 (2H, qui, *J*=7.7 Hz), 1.36 (2H, sext, *J*=7.7 Hz), 0.91 (3H, t, *J*=7.4 Hz) ppm. ¹³C NMR (600 MHz, DMSO-*d*₆): δ= 166.58, 157.83, 139.13, 132.03, 128.65, 122.20, 120.71, 118.15, 111.73, 63.64, 55.65, 30.29, 18.67, 13.57 ppm.

(E)-Butyl 3-(4-acetylphenyl)acrylate (3j)²²



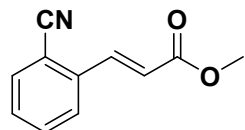
Transparent oil, 84%. ^1H NMR (600 MHz, DMSO- d_6): $\delta = 7.97$ (2H, d, $J=8.3$ Hz), 7.87 (2H, d, $J=8.3$ Hz), 7.70 (1H, d, $J=15.9$ Hz), 6.78 (1H, d, $J=15.9$ Hz), 4.16 (2H, t, $J=6.6$ Hz), 2.60 (3H, s), 1.63 (2H, m), 1.38 (2H, m), 0.92 (3H, t, $J=7.4$ Hz) ppm. ^{13}C NMR (600 MHz, DMSO- d_6): $\delta = 197.43, 165.98, 143.01, 138.31, 137.69, 128.63, 128.54, 120.63, 63.92, 30.24, 26.81, 18.65, 13.56$ ppm.

(E)-Methyl 3-(2-nitrophenyl)acrylate (3l)²²



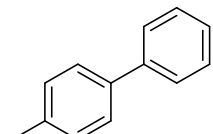
Yellow solid, 82%. ^1H NMR (600 MHz, DMSO- d_6): $\delta = 8.08$ (1H, d, $J=8.2$ Hz), 7.93 (2H, m), 7.78 (1H, t, $J=7.4$ Hz), 7.68 (1H, t, $J=7.6$ Hz), 6.64 (1H, d, $J=15.9$ Hz), 3.75 (3H, s) ppm. ^{13}C NMR (600 MHz, DMSO- d_6): $\delta = 165.96, 148.27, 139.65, 133.91, 131.03, 129.33, 129.20, 124.71, 122.27, 51.80$ ppm.

(E)-methyl-3-(2-cyanophenyl)acrylate (3m)²³



White solid, 67%. ^1H NMR (600 MHz, DMSO- d_6): $\delta = 8.11$ (1H, d, $J=7.7$ Hz), 7.92 (1H, d, $J=7.7$ Hz), 7.80 (1H, d, $J=15.9$ Hz), 7.77 (1H, t, $J=7.7$ Hz), 7.62 (1H, t, $J=7.7$ Hz), 6.90 (1H, d, $J=15.9$ Hz), 3.77 (3H, s) ppm. ^{13}C NMR (600 MHz, DMSO- d_6): $\delta = 165.97, 138.94, 136.31, 133.64, 133.50, 130.85, 127.44, 122.58, 117.18, 111.70, 51.89$ ppm.

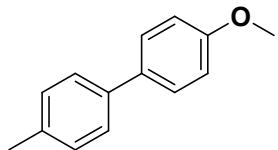
4-methylbiphenyl (6a, 6c)²⁴



White solid, 90%. ^1H NMR (600 MHz, DMSO- d_6): $\delta = 7.63$ (2H, d, $J=7.6$ Hz), 7.55 (2H, d, $J=7.6$ Hz), 7.45 (2H, t, $J=7.6$ Hz), 7.34 (1H, d, $J=7.3$ Hz), 7.27 (2H, d, $J=7.6$ Hz), 2.34 (3H,

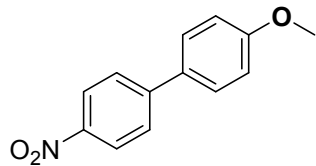
s) ppm. ^{13}C NMR (600 MHz, DMSO- d_6): δ = 140.08, 137.29, 136.69, 129.51, 128.87, 127.10, 126.50, 126.41, 20.65 ppm.

4-methoxy-4'-methylbiphenyl (6b**)²⁵**



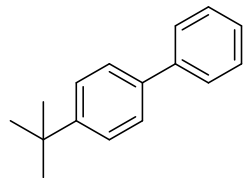
White solid, 94%. ^1H NMR (600 MHz, DMSO- d_6): δ = 7.55 (2H, m), 7.49 (2H, d, J =7.7 Hz), 7.22 (2H, d, J =8.2 Hz), 6.99 (2H, m), 3.78 (3H, s), 2.32 (3H, s) ppm. ^{13}C NMR (600 MHz, DMSO- d_6): δ = 158.66, 136.96, 135.84, 132.48, 129.43, 127.44, 125.97, 114.28, 55.10, 20.59 ppm.

4-methoxy-4'-nitrobiphenyl (6d**)²⁶**



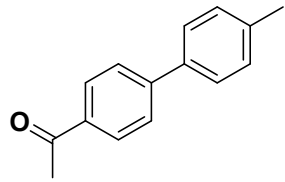
Yellow solid, 95%. ^1H NMR (600 MHz, DMSO- d_6): δ = 8.26 (2H, d, J =8.8 Hz), 7.91 (2H, d, J =8.8 Hz), 7.76 (2H, d, J =8.8 Hz), 7.09 (2H, d, J =8.8 Hz), 3.82 (3H, s) ppm. ^{13}C NMR (600 MHz, DMSO- d_6): δ = 160.18, 146.28, 145.99, 129.91, 128.56, 126.99, 124.08, 114.68, 55.31 ppm.

4-tert-butylbiphenyl (6e**)²⁷**



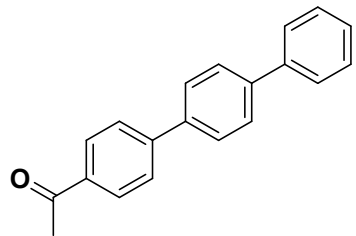
White solid, 80%. ^1H NMR (600 MHz, DMSO- d_6): δ = 7.64 (2H, m), 7.58 (2H, m), 7.48 (2H, m), 7.45 (2H, m), 7.34 (1H, m), 1.31 (9H, s) ppm. ^{13}C NMR (600 MHz, DMSO- d_6): δ = 149.82, 140.08, 137.34, 128.86, 127.13, 126.50, 126.35, 125.68, 34.22, 31.09 ppm.

1-(4'-methylbiphenyl-4-yl)ethanone (6f**)²⁵**



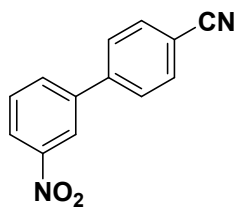
White solid, 90%. ¹H NMR (600 MHz, DMSO-*d*₆): δ=8.01 (2H, d, *J*=7.5 Hz), 7.79 (2H, d, *J*=7.4 Hz), 7.64 (2H, d, *J*=8.3 Hz), 7.31 (2H, d, *J*=8.3 Hz), 2.60 (3H, s), 2.36 (3H, s) ppm. ¹³C NMR (600 MHz, DMSO-*d*₆): δ= 197.43, 144.43, 137.90, 135.97, 135.36, 129.68, 128.88, 126.80, 126.51, 26.72, 20.71 ppm.

1-(1,1':4',1''-terphenyl-4-yl)ethanone (6g**)²⁸**



White solid, 88%. ¹H NMR (600 MHz, DMSO-*d*₆): δ= 8.06 (2H, d, *J*=7.9 Hz), 7.89 (2H, m), 7.87 (2H, m), 7.82 (2H, m), 7.74 (2H, m), 7.50 (2H, t, *J*=7.5 Hz), 7.41 (1H, t, *J*=7.4 Hz), 2.63 (3H, s) ppm. ¹³C NMR (600 MHz, DMSO-*d*₆): δ = 197.52, 143.94, 140.08, 139.40, 137.82, 135.69, 129.05, 128.98, 127.76, 127.55, 127.35, 126.74, 126.67, 26.81 ppm.

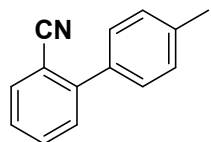
3'-nitrobiphenyl-4-carbonitrile (6h**)²⁹**



Light yellow solid, 60%. ¹H NMR (600 MHz, DMSO-*d*₆): δ=8.51 (1H, t), 8.29 (1H, d, *J*=8.2 Hz), 8.22 (1H, d, *J*=7.8 Hz), 8.00 (4H, m), 7.81 (1H, t, *J*=7.9 Hz) ppm. ¹³C NMR (600 MHz,

DMSO-*d*₆): δ= 148.47, 142.24, 139.84, 133.68, 133.04, 130.72, 128.06, 123.34, 121.70, 118.60, 111.18 ppm.

4'-methylbiphenyl-2-carbonitrile (6i**)³⁰**

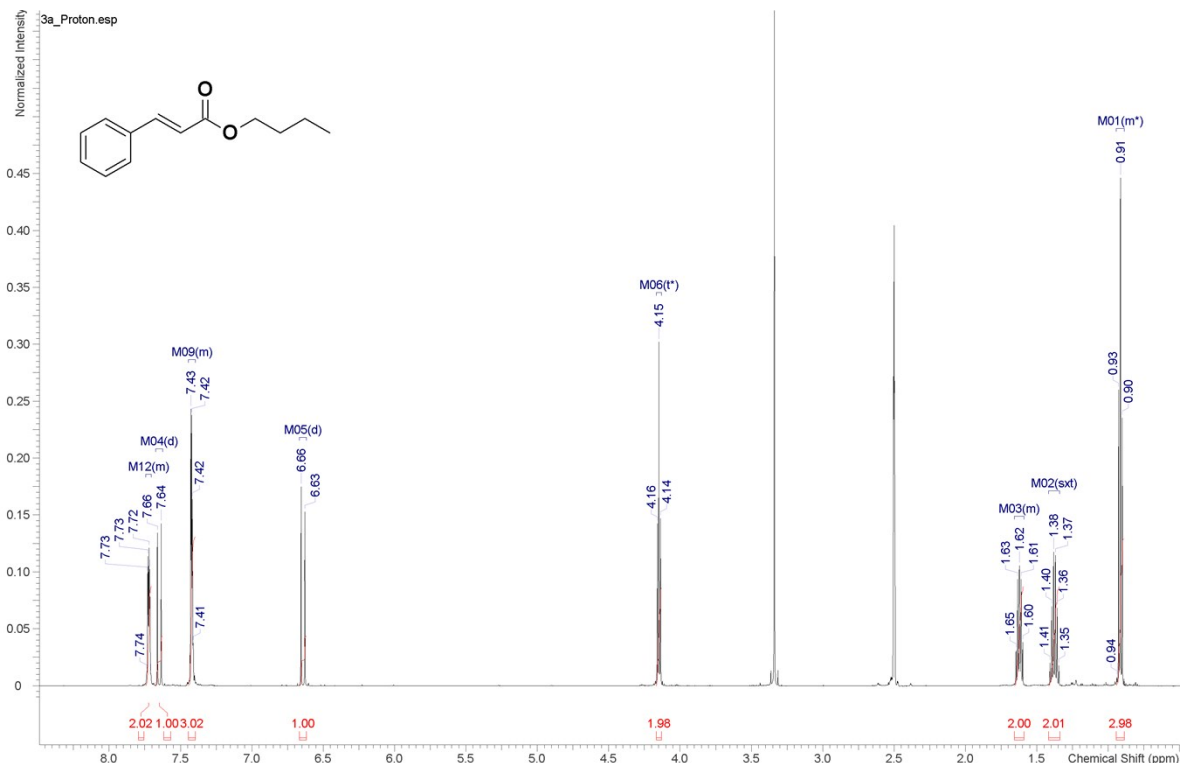


White solid, 82%. ¹H NMR (600 MHz, DMSO-*d*₆): δ= 7.92 (1H, dd, *J*=7.7 Hz, *J*=1.1 Hz), 7.76 (1H, td, *J*=7.7 Hz, *J*=1.1 Hz), 7.59 (1H, d, *J*=7.7 Hz), 7.55 (1H, td, *J*=7.7 Hz, *J*=1.1 Hz), 7.46 (2H, d, *J*=8.3 Hz), 7.33 (2H, d, *J*=8.3 Hz), 2.38 (3H, s) ppm. ¹³C NMR (600 MHz, DMSO-*d*₆): δ= 144.54, 138.26, 134.97, 133.81, 133.46, 129.98, 129.29, 128.55, 127.93, 118.64, 110.08, 20.75 ppm.

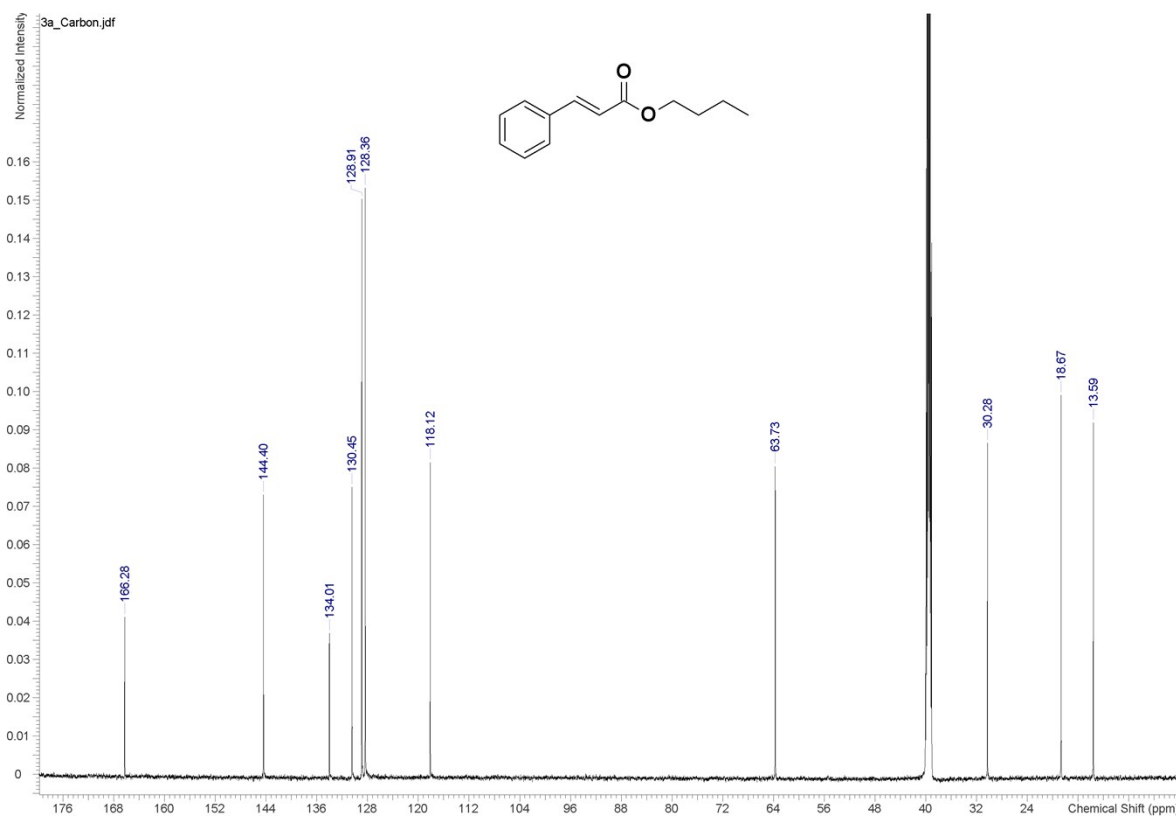
¹H and ¹³C NMR spectra of compounds

(E)-Butyl cinnamate (3a)

¹HNMR

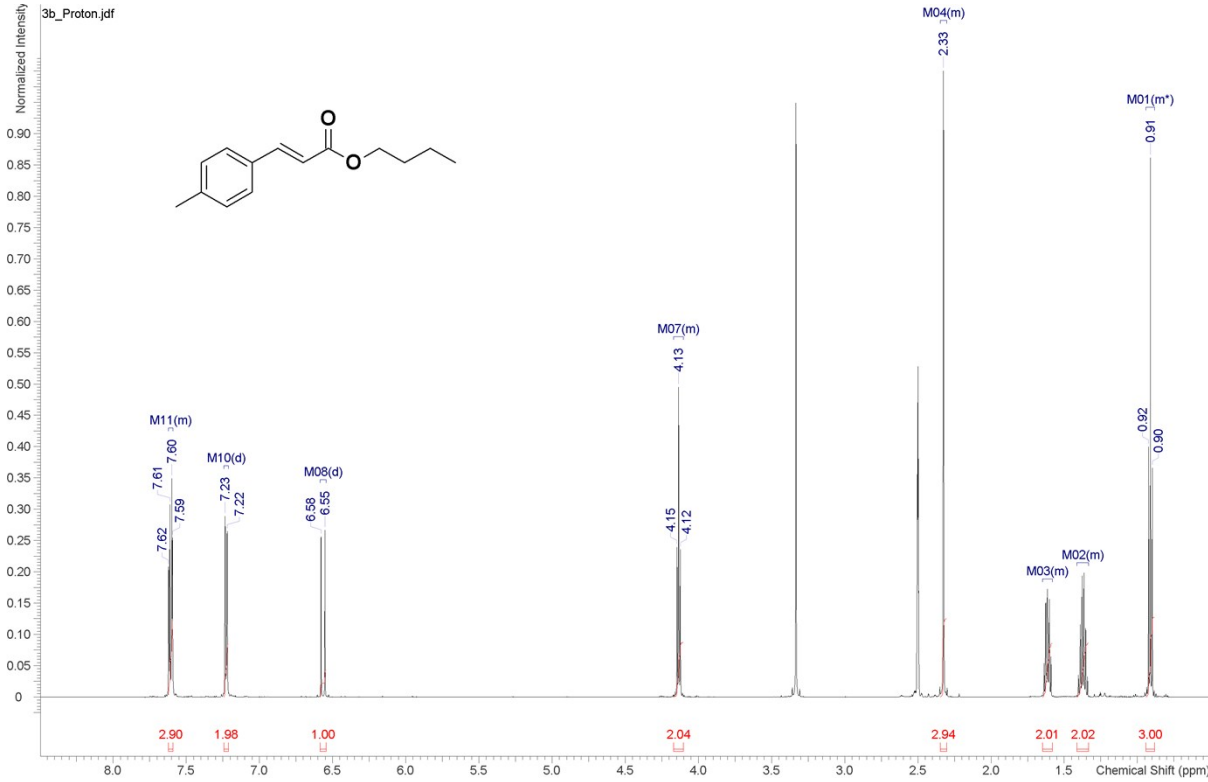


¹³CNMR

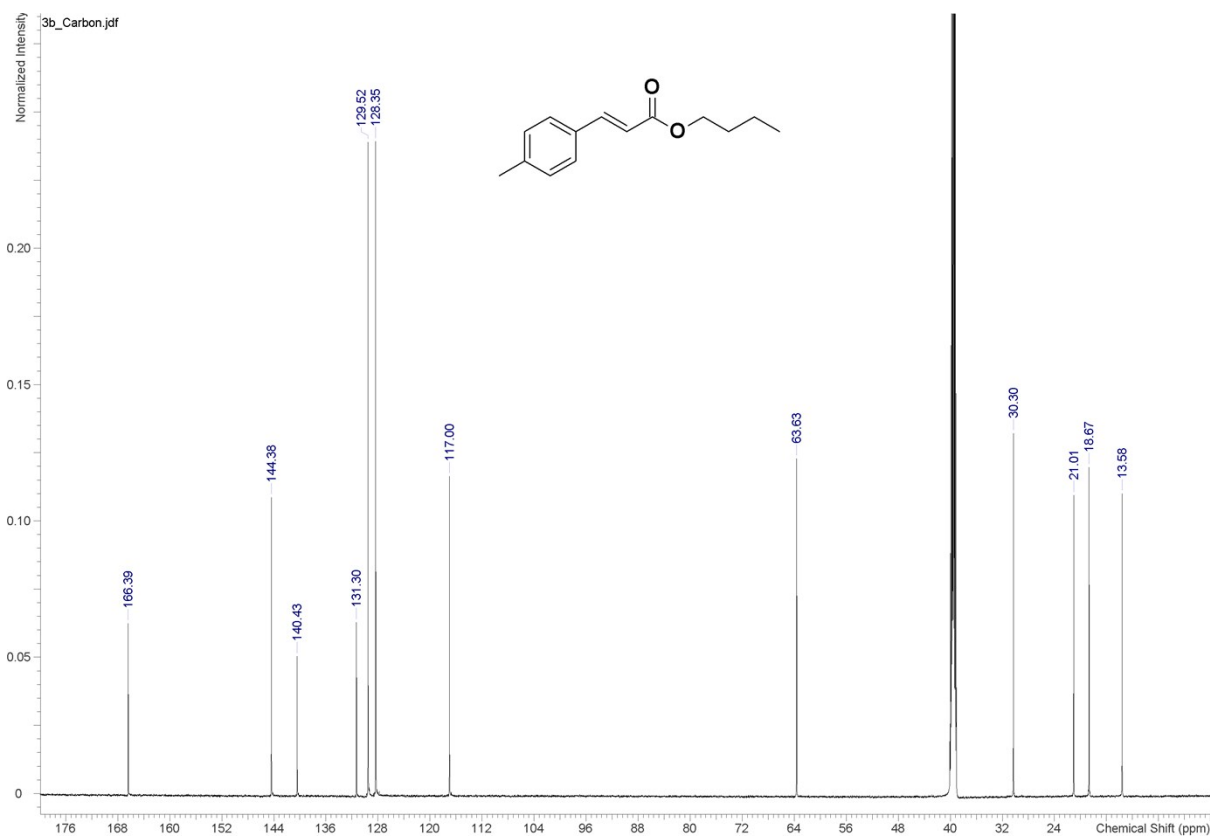


(E)-Butyl 3-p-tolylacrylate (3b)

¹H NMR

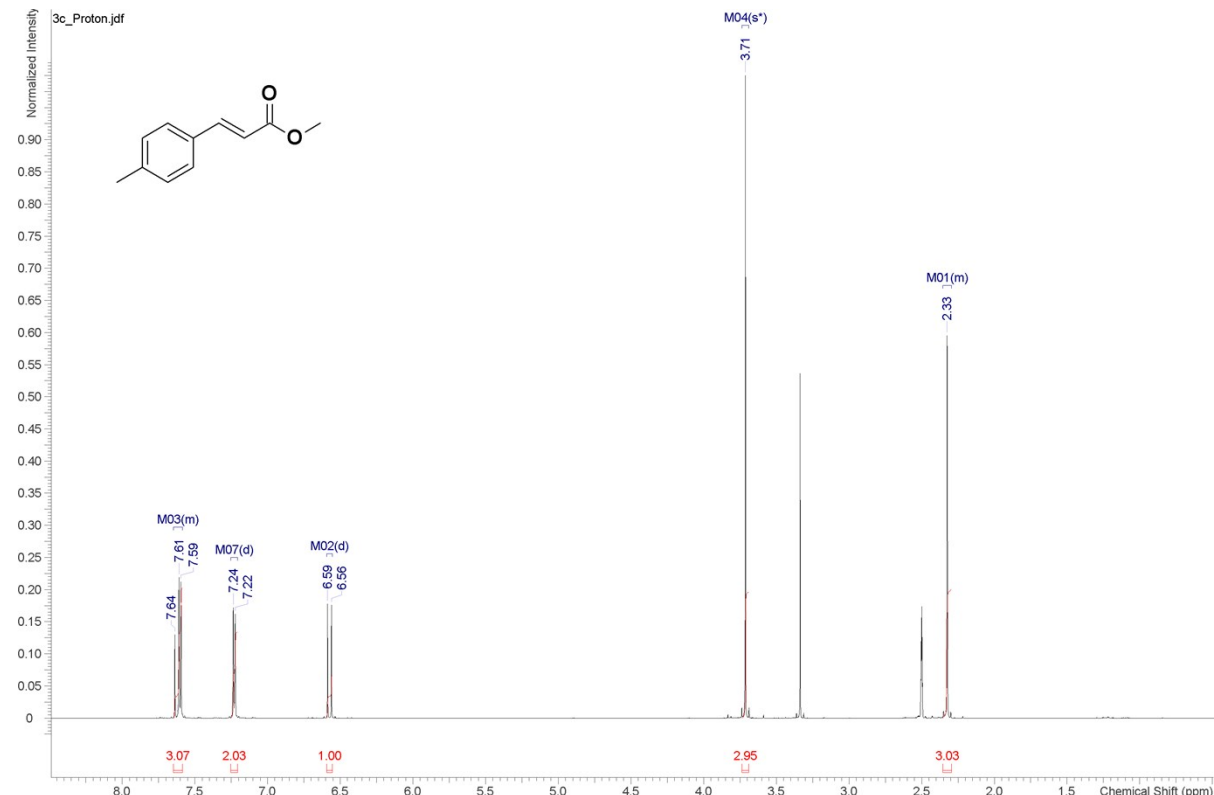


¹³C NMR

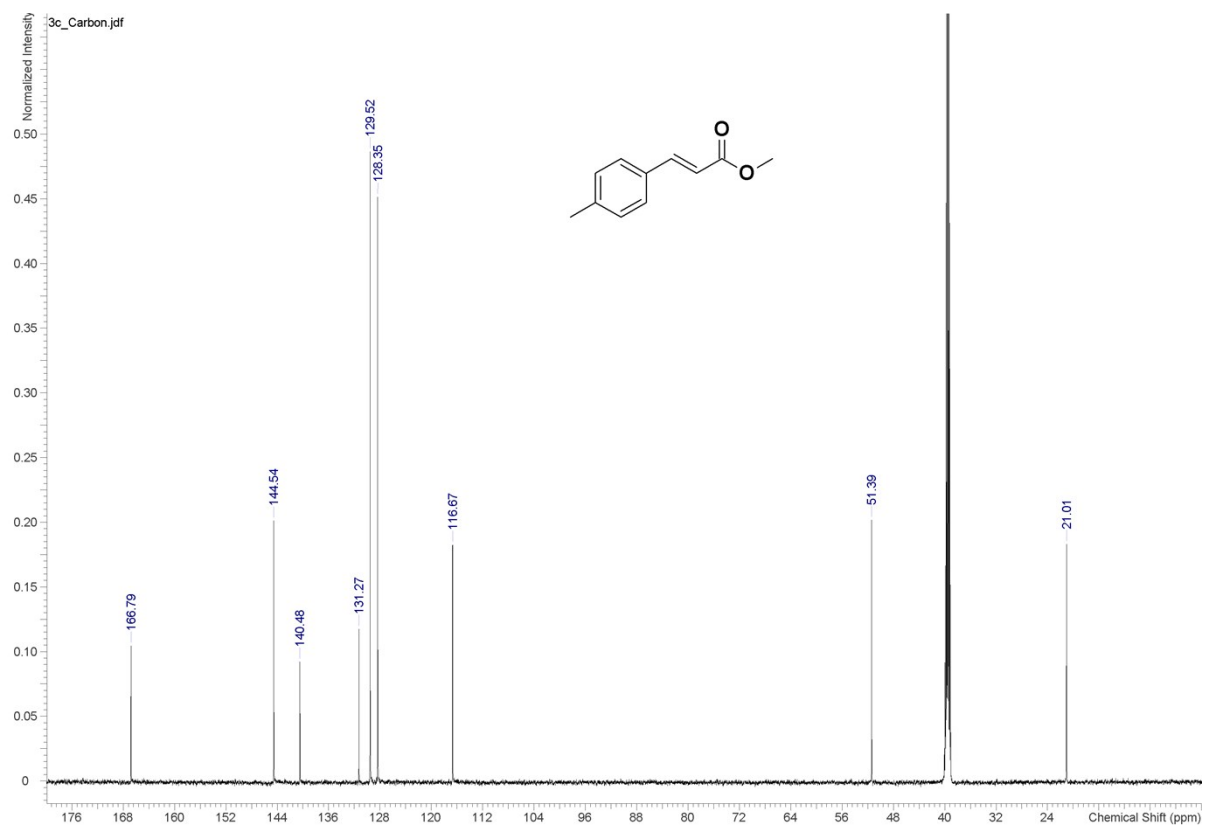


(E)-Methyl 3-p-tolylacrylate (3c)

¹H NMR

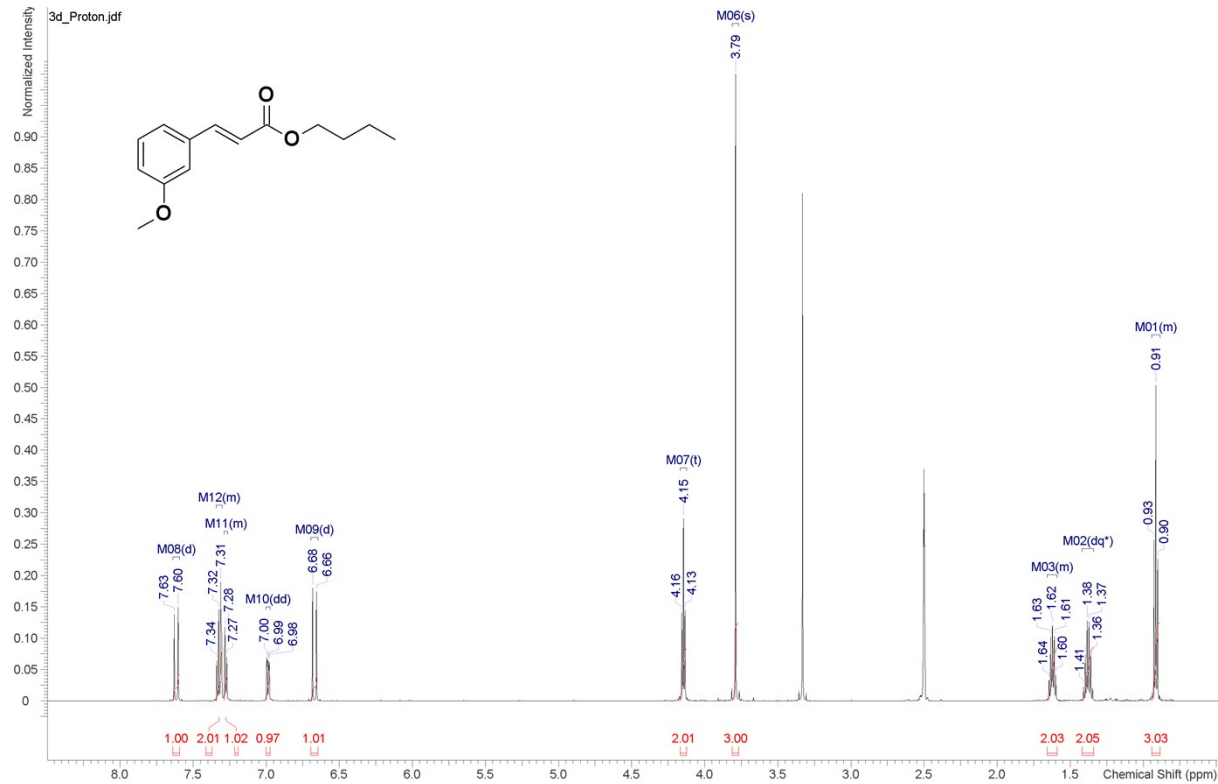


¹³C NMR

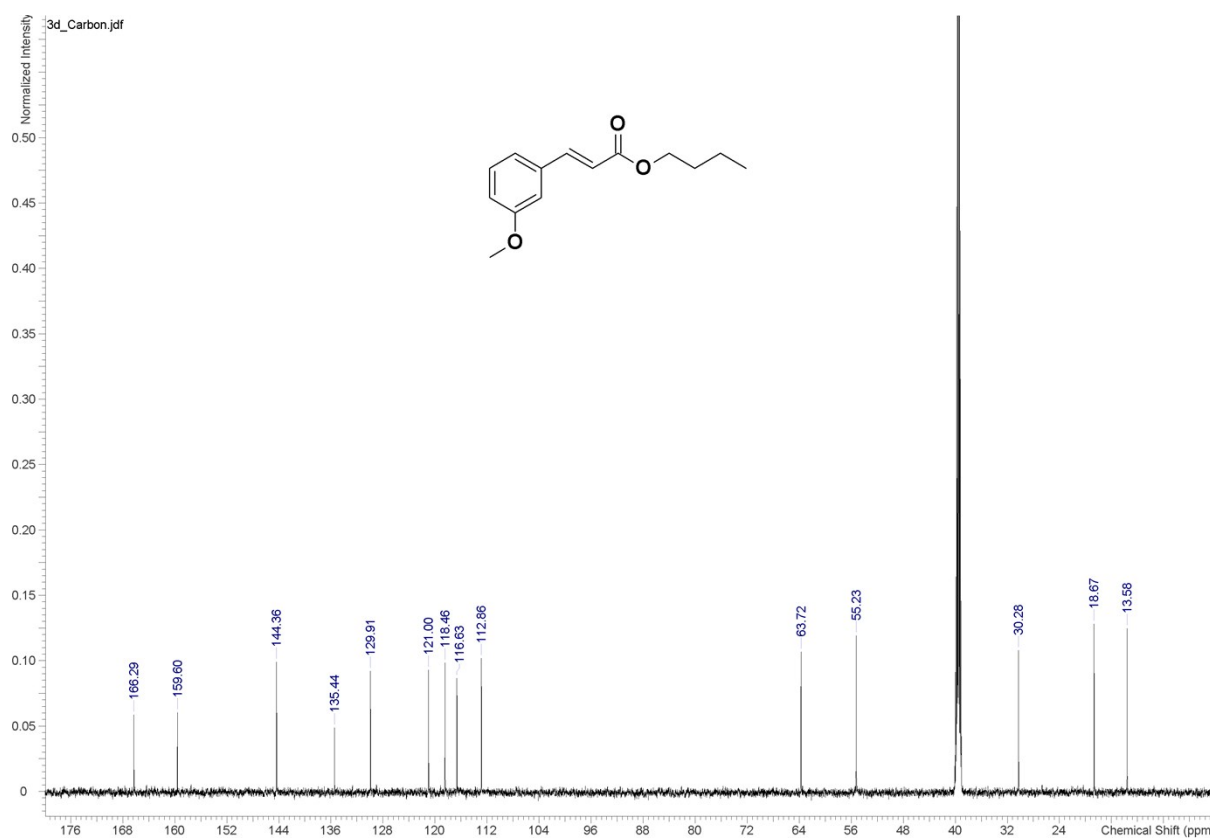


(E)-Butyl 3-(3-methoxyphenyl)acrylate (3d)

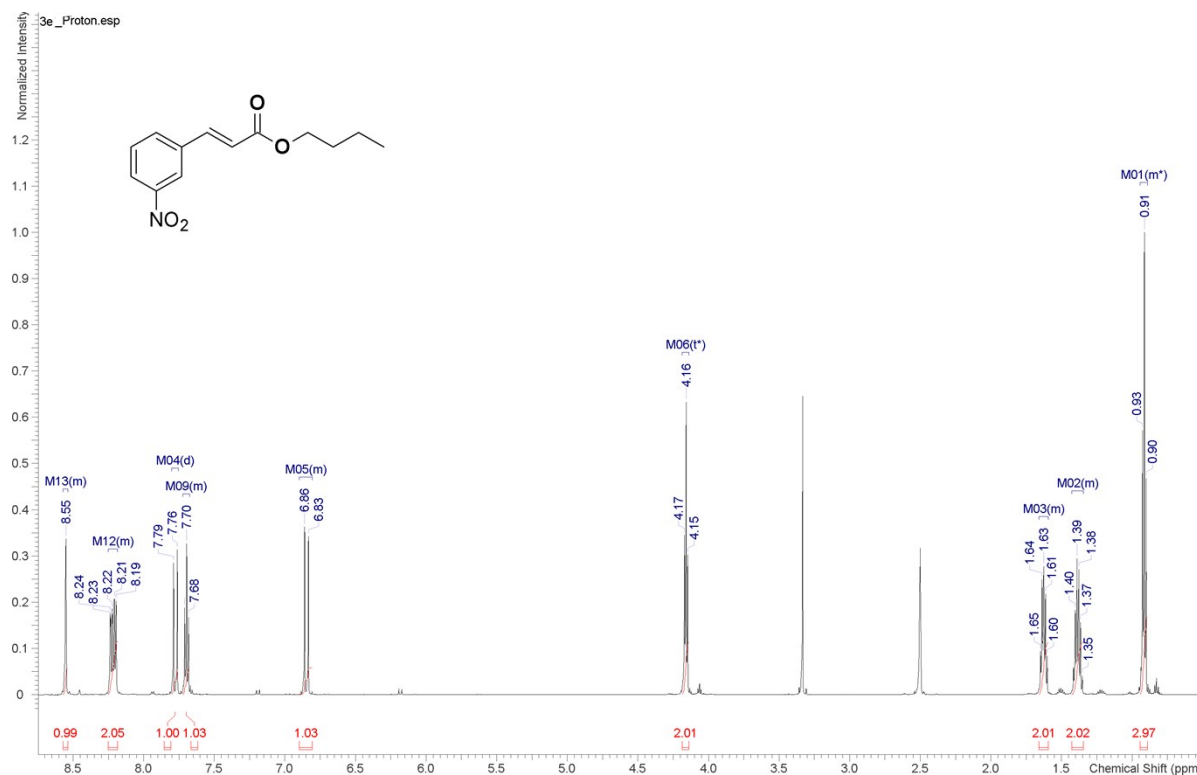
¹H NMR



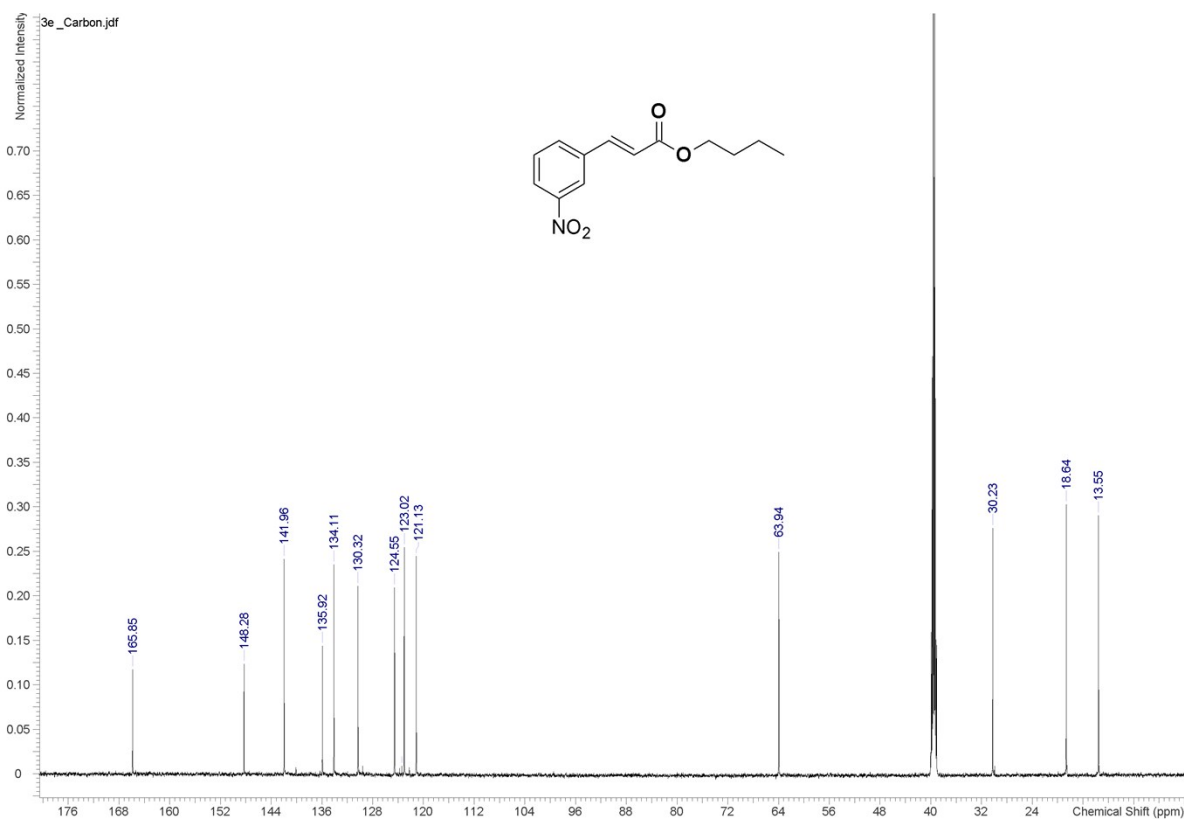
¹³C NMR



¹H NMR

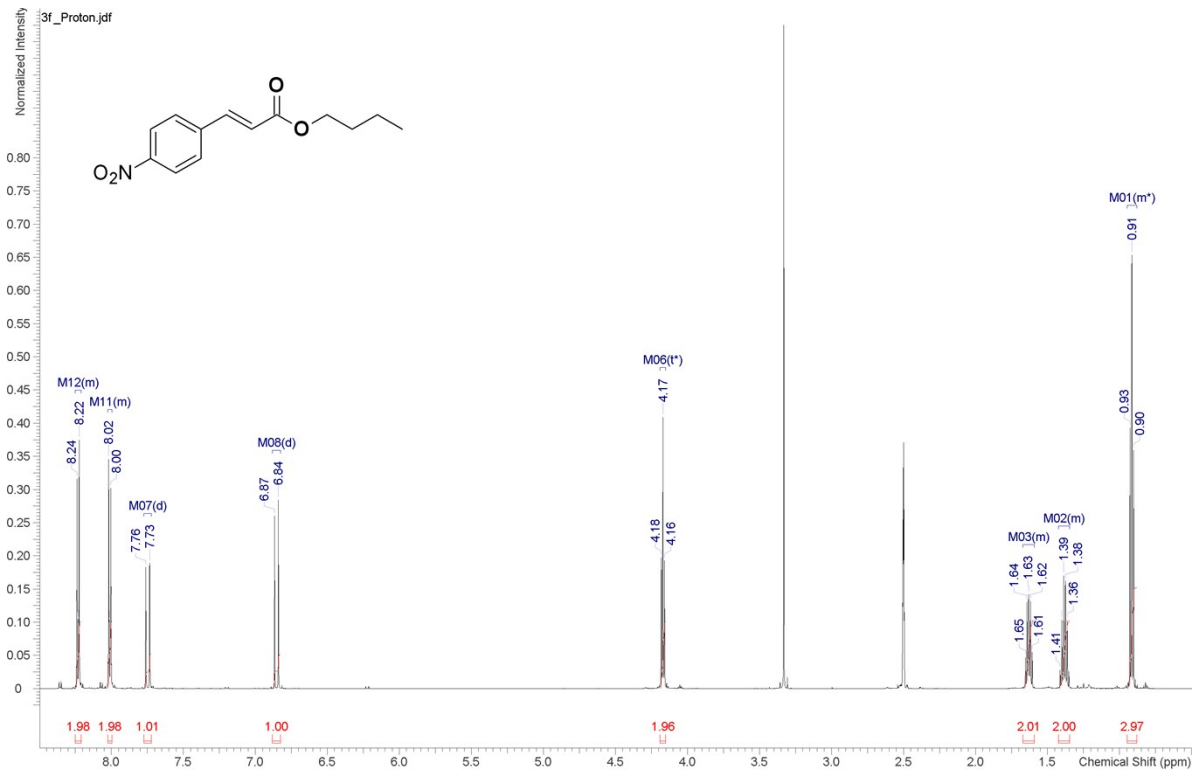


¹³C NMR

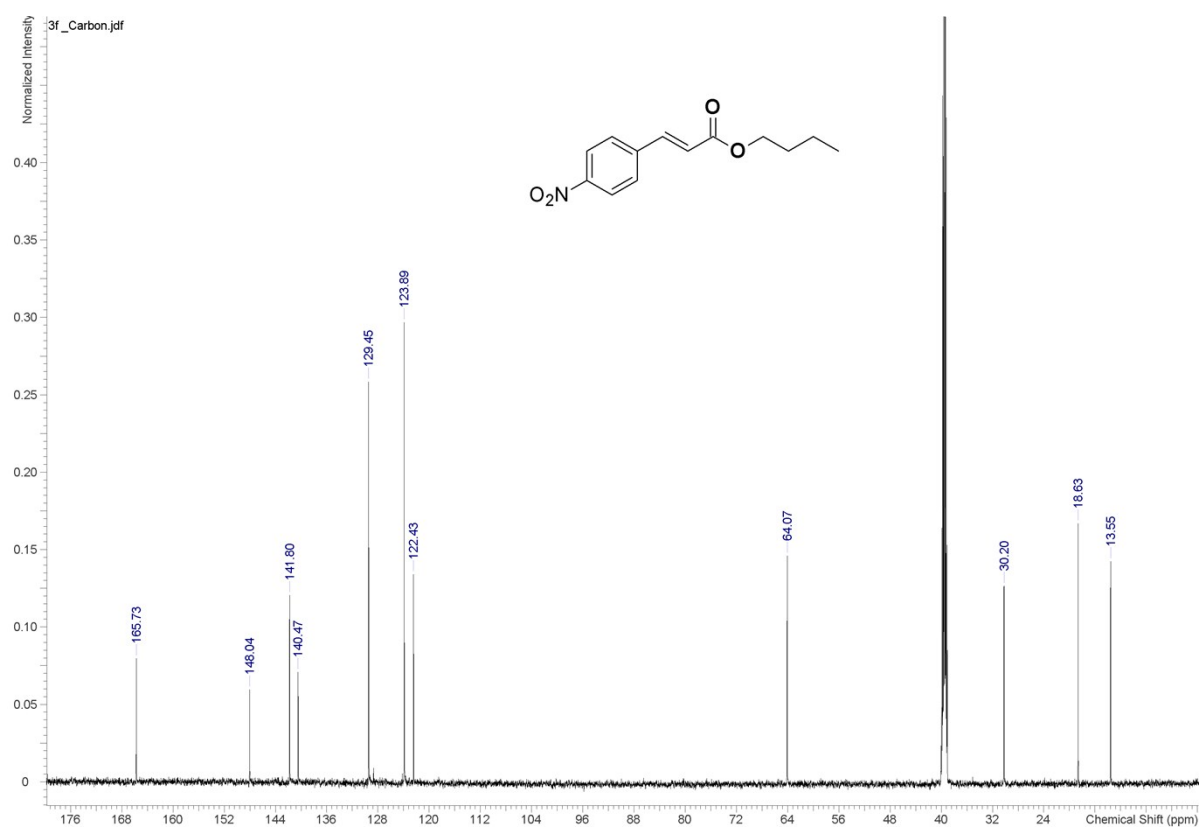


(E)-Butyl 3-(4-nitrophenyl)acrylate (3f)

¹H NMR

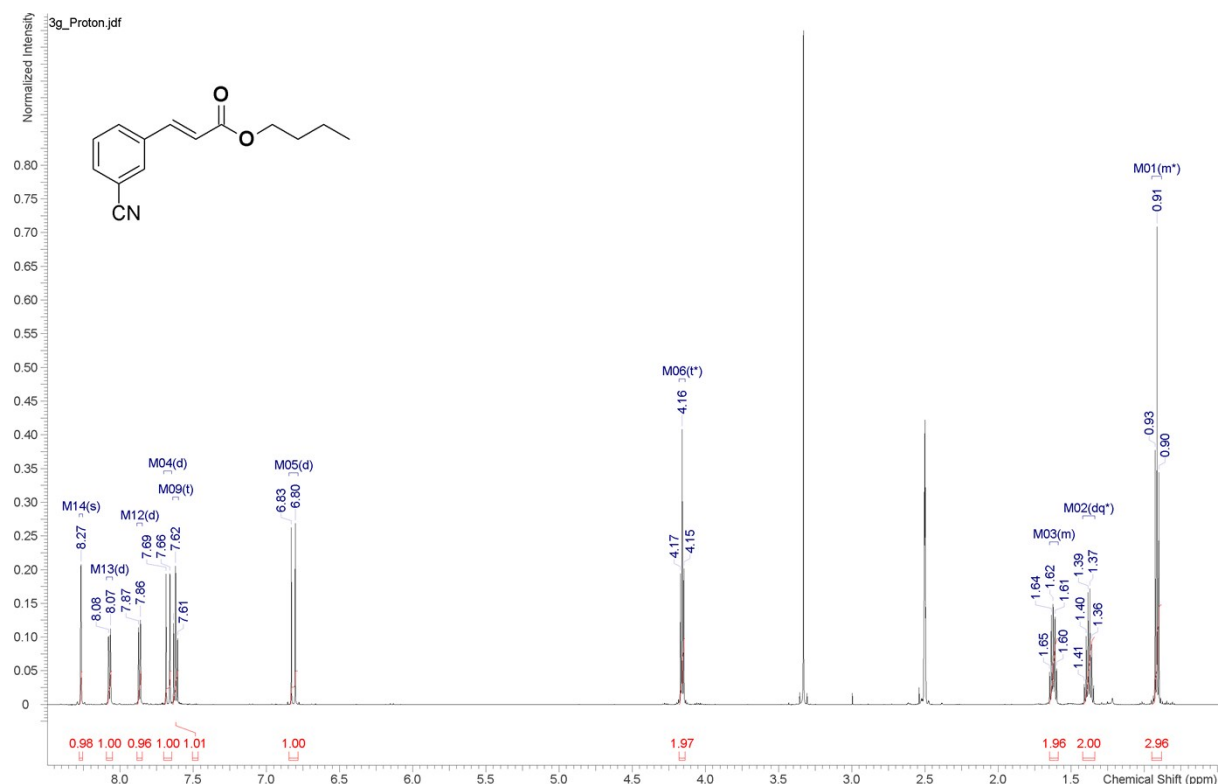


¹³CNMR

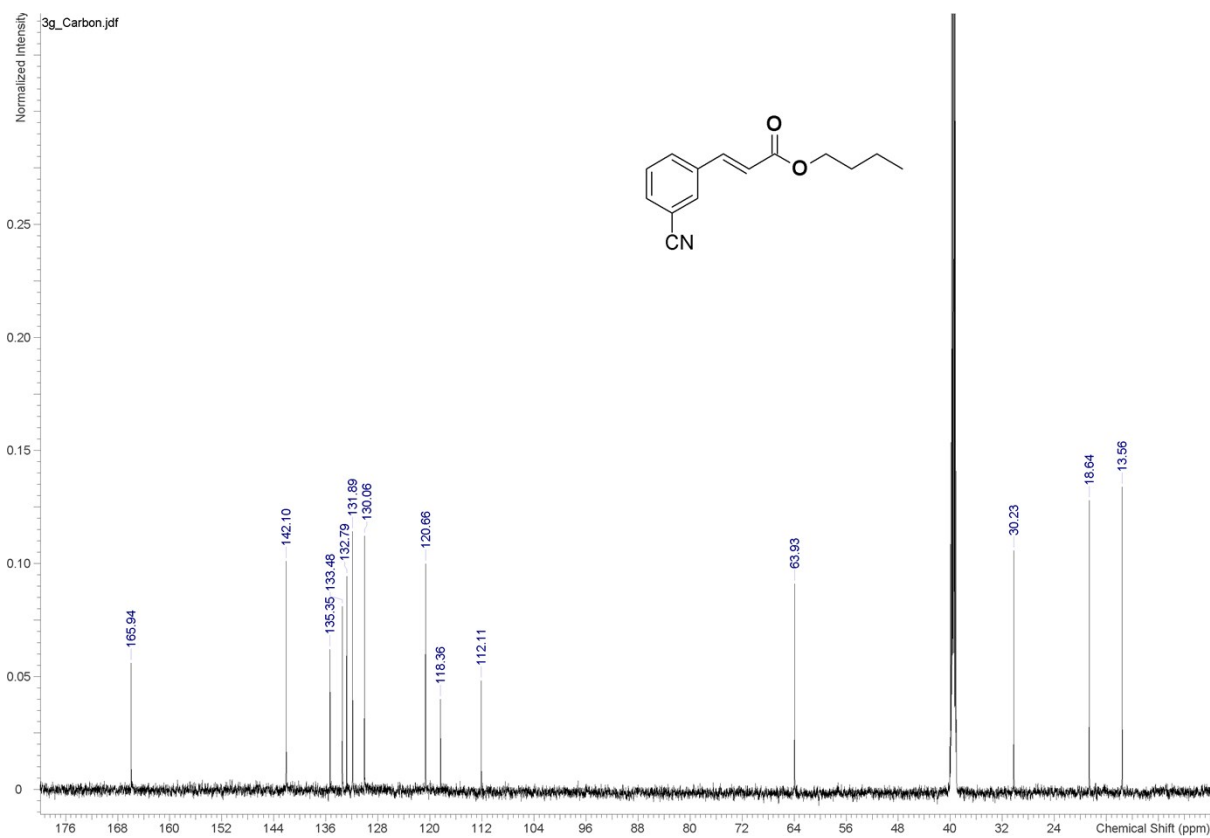


(E)-Butyl 3-(3-cyanophenyl)acrylate (3g)

¹H NMR

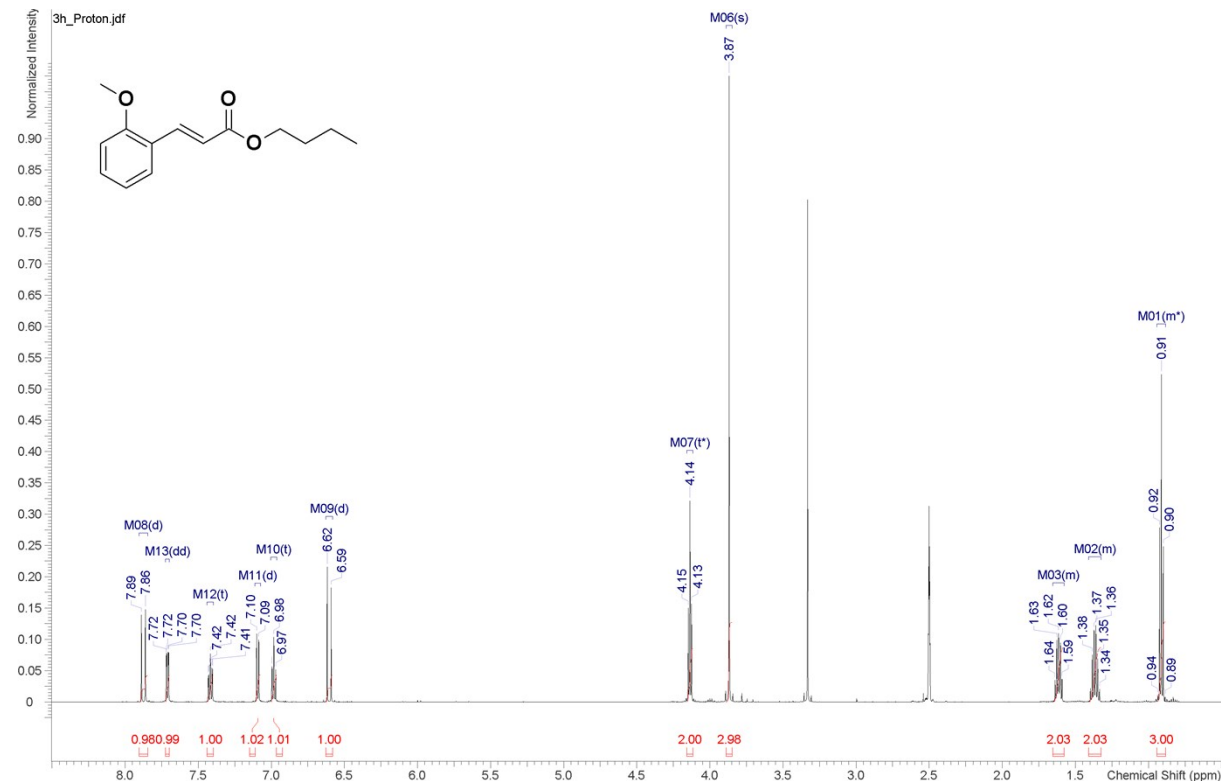


¹³CNMR

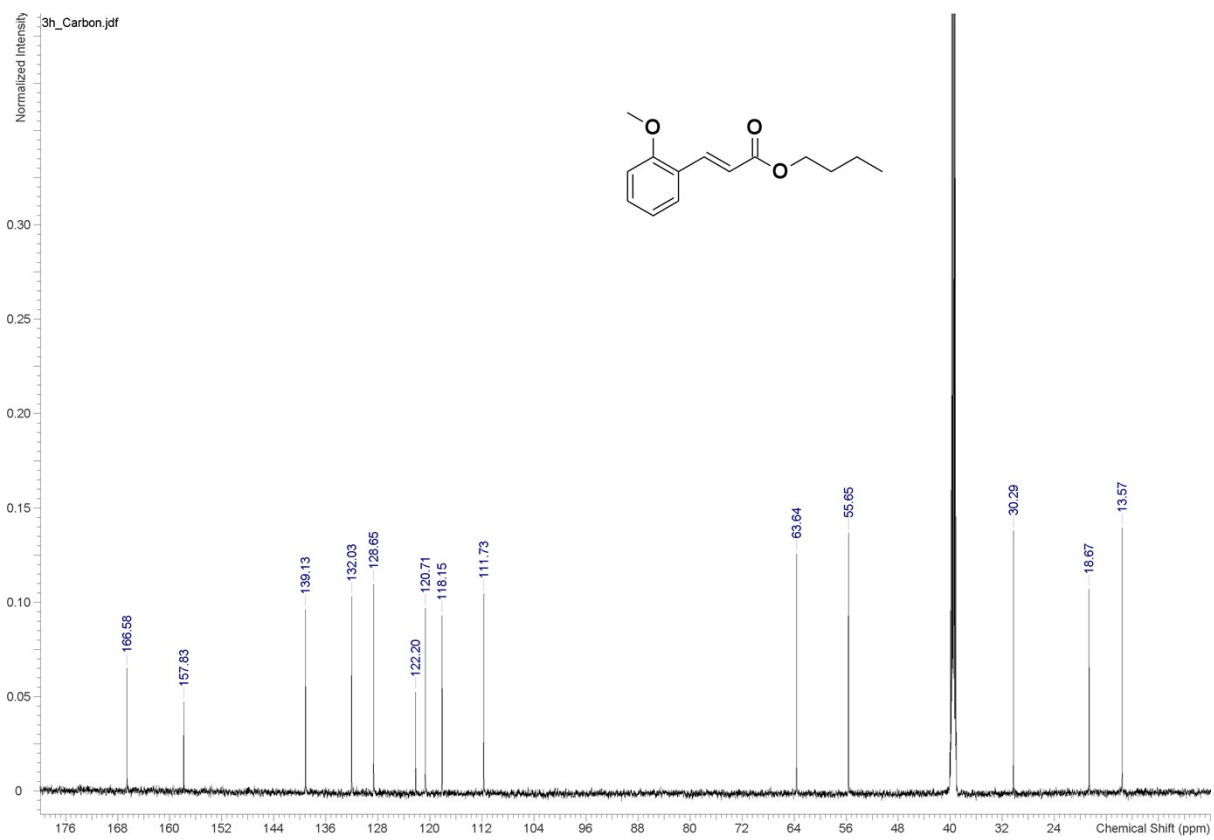


(E)-Butyl 3-(2-methoxyphenyl)acrylate (3h)

¹H NMR

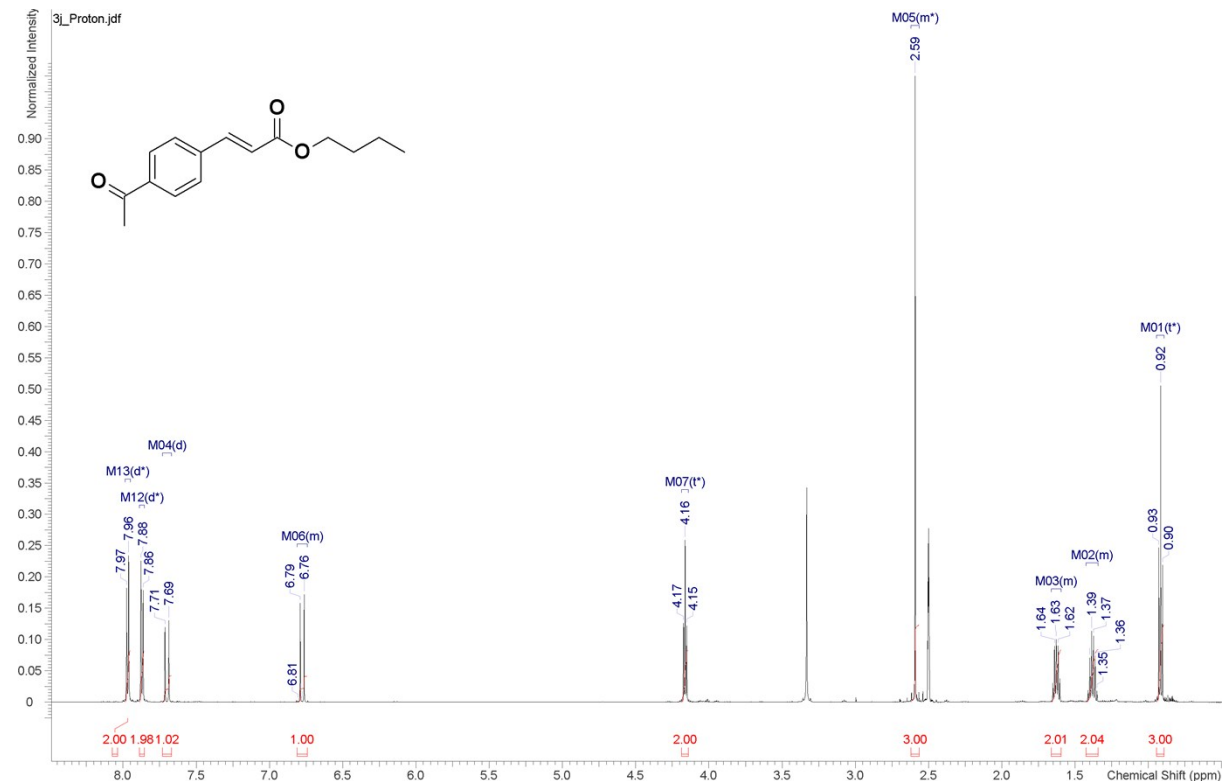


¹³C NMR

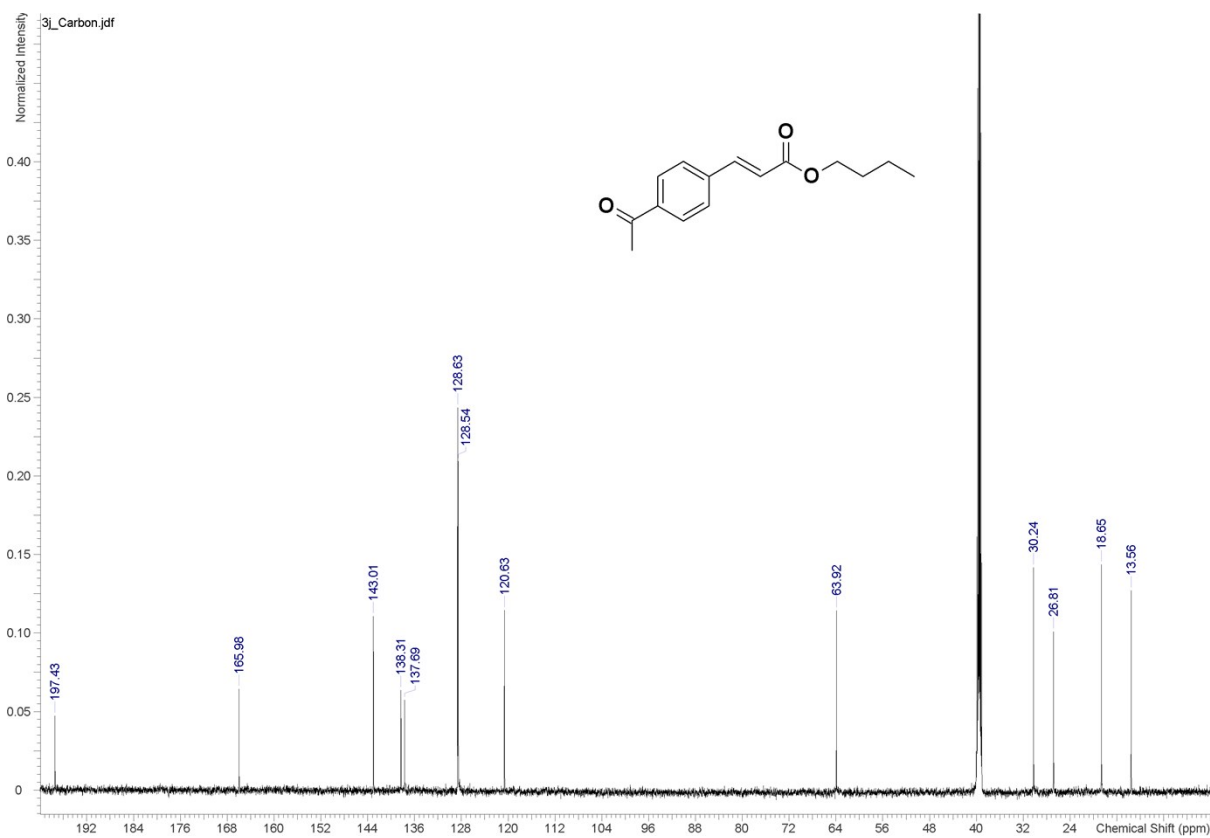


(E)-Butyl 3-(4-acetylphenyl)acrylate (3j)

¹H NMR

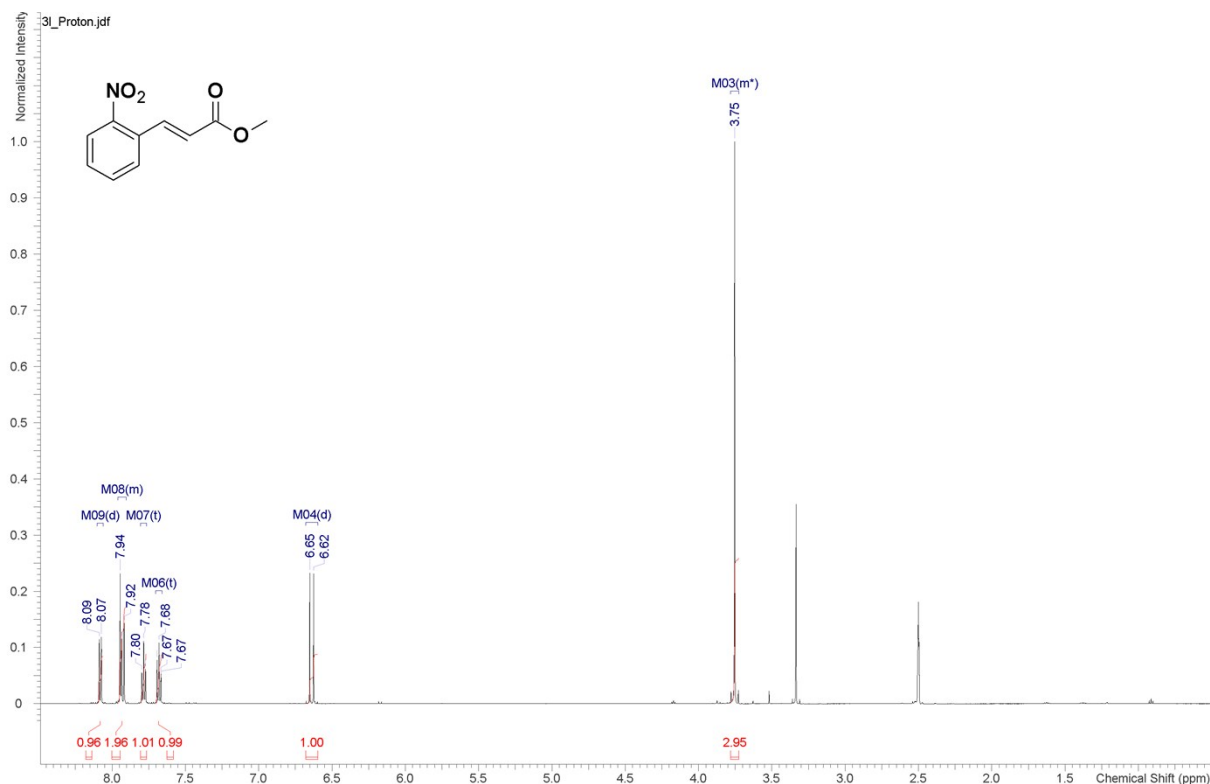


¹³C NMR

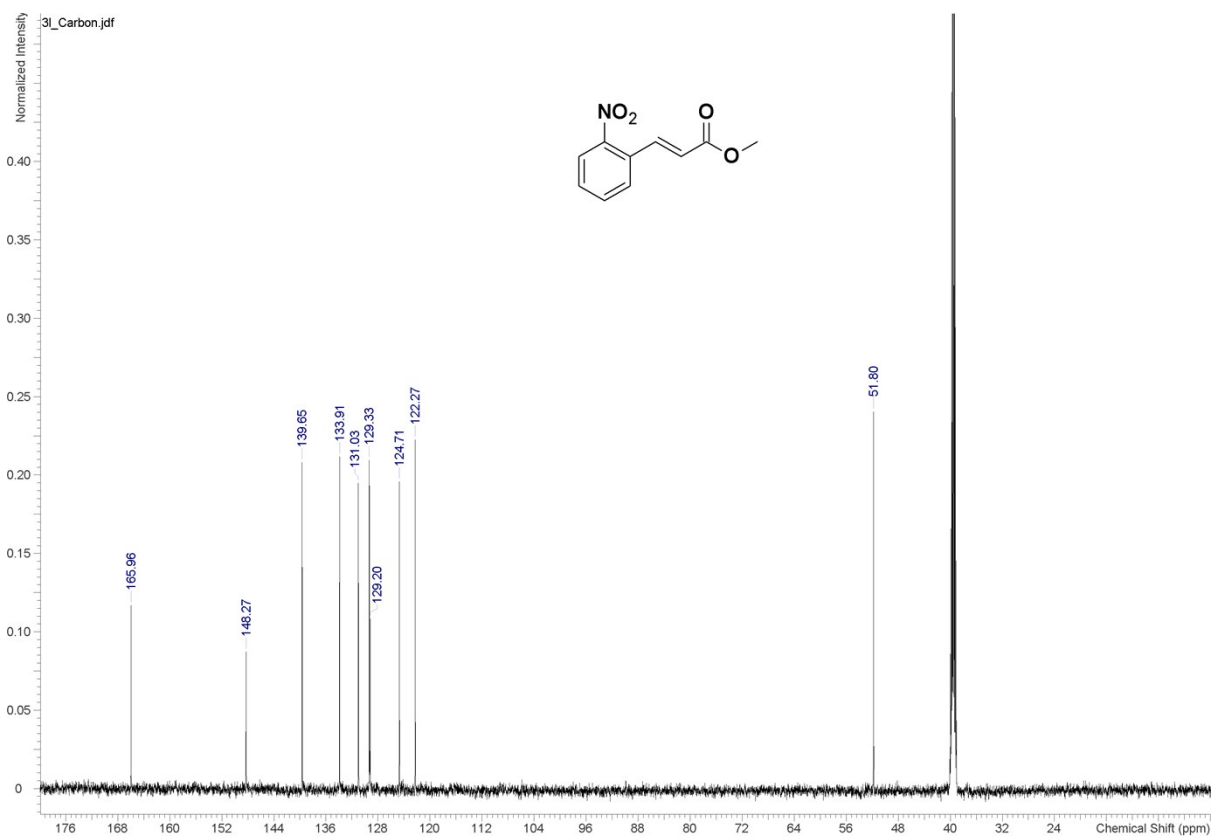


(E)-Methyl 3-(2-nitrophenyl)acrylate (3l)

¹H NMR

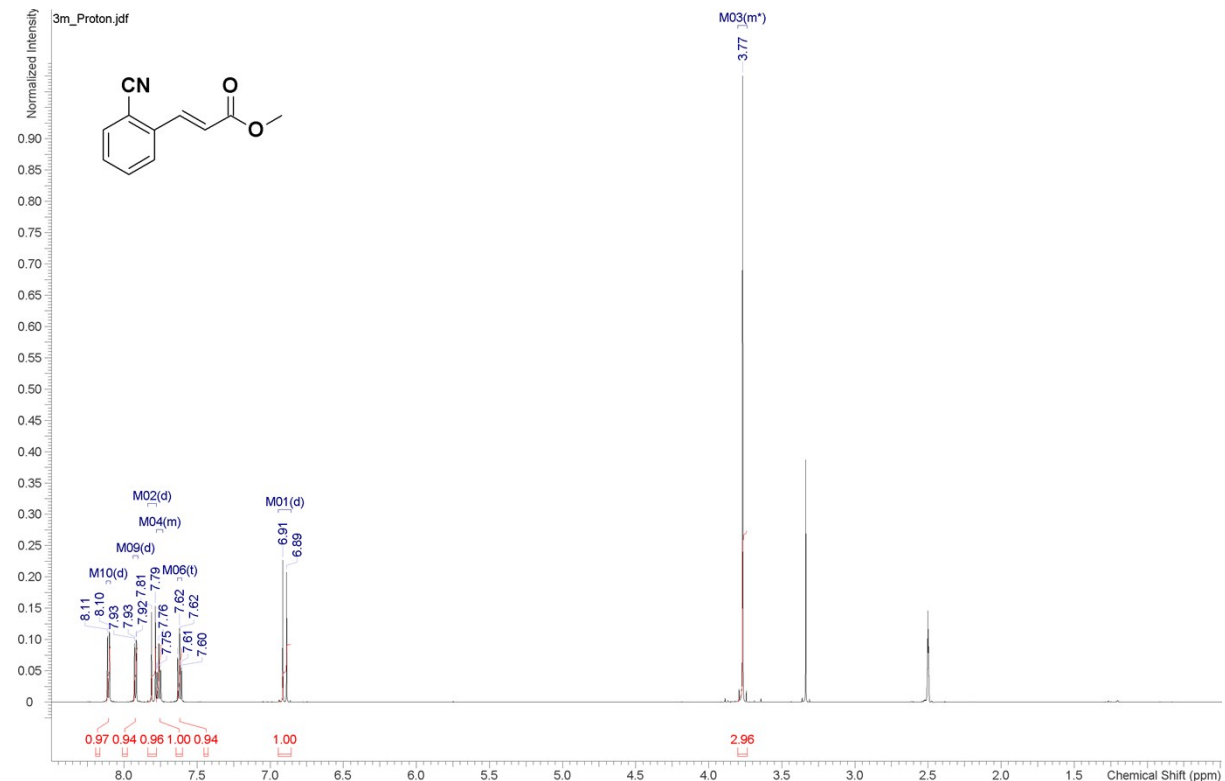


¹³C NMR

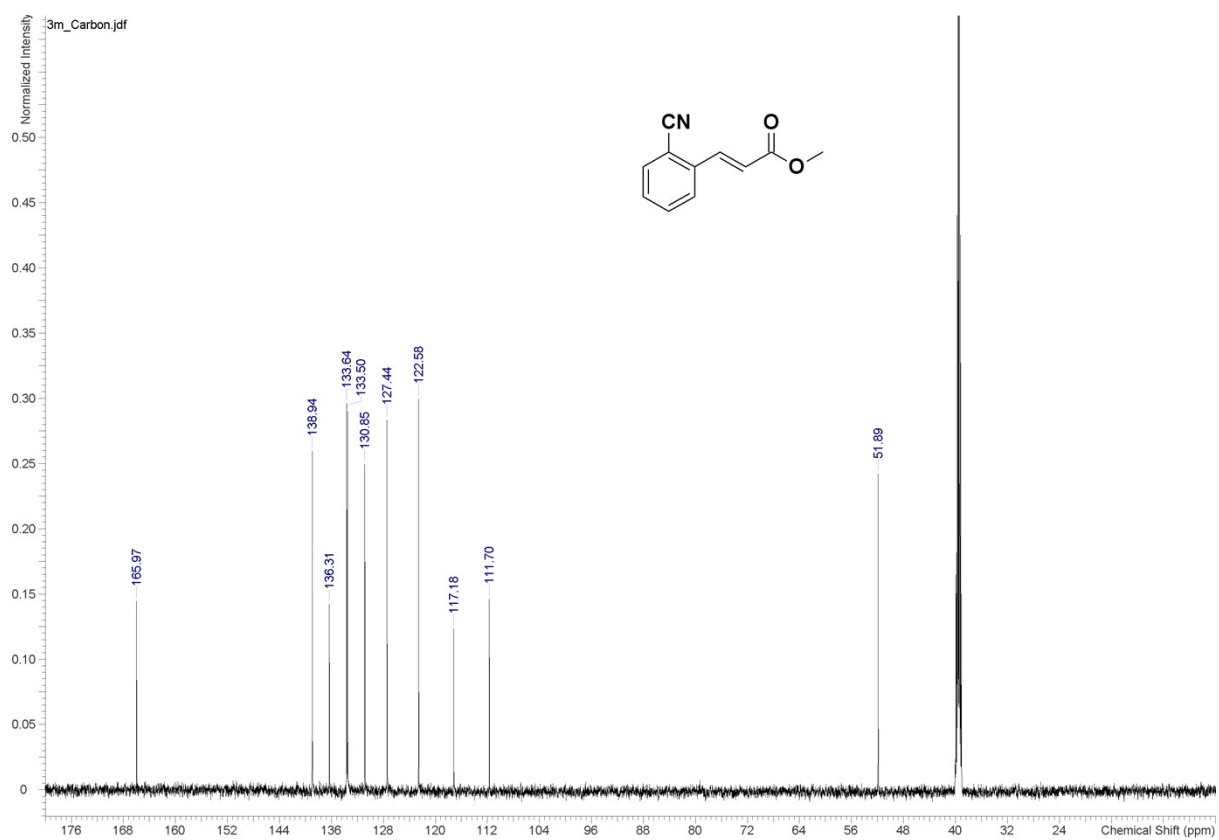


(E)-methyl-3-(2-cyanophenyl)acrylate (3m)

¹H NMR

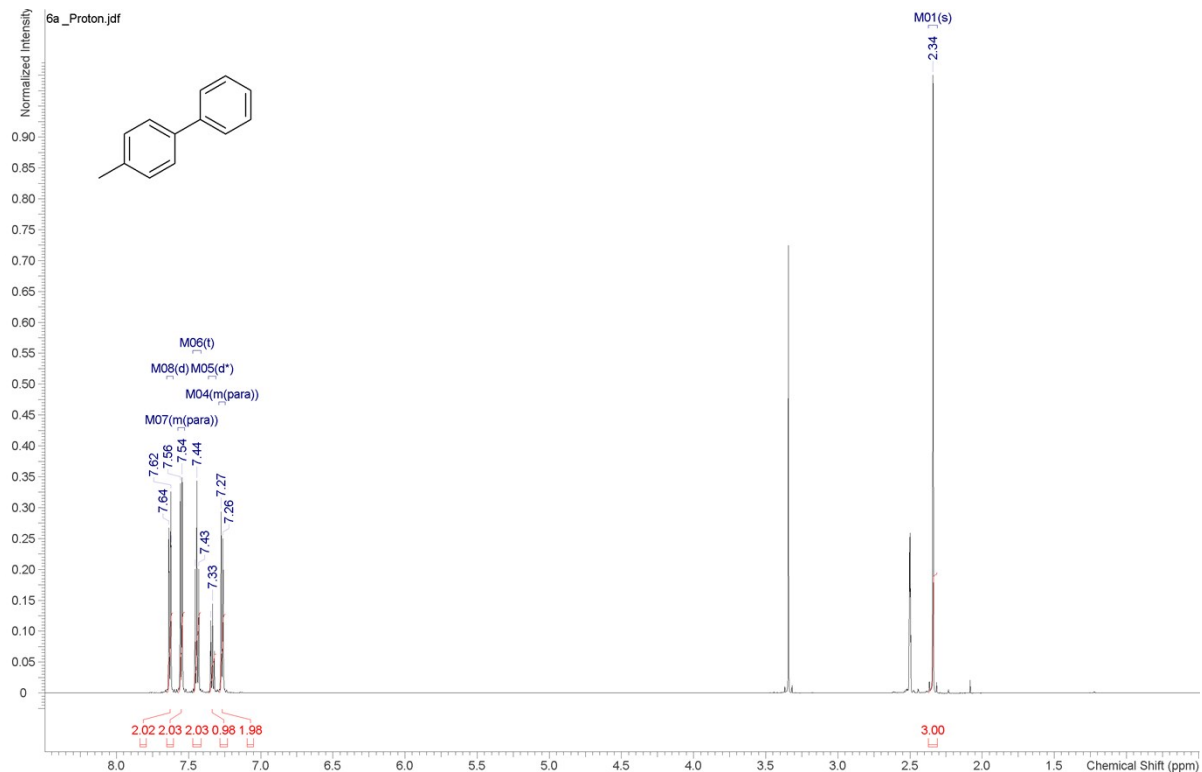


¹³C NMR

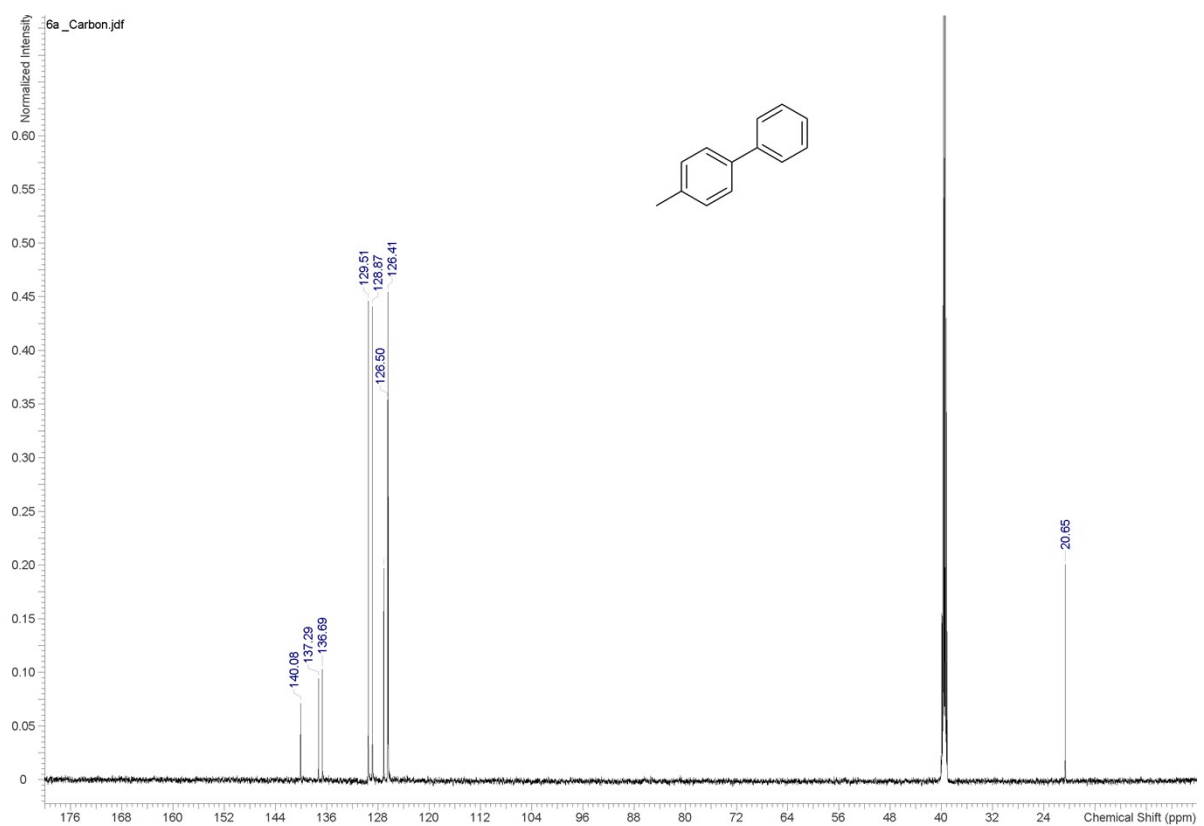


4-methylbiphenyl (**6a**)

¹H NMR

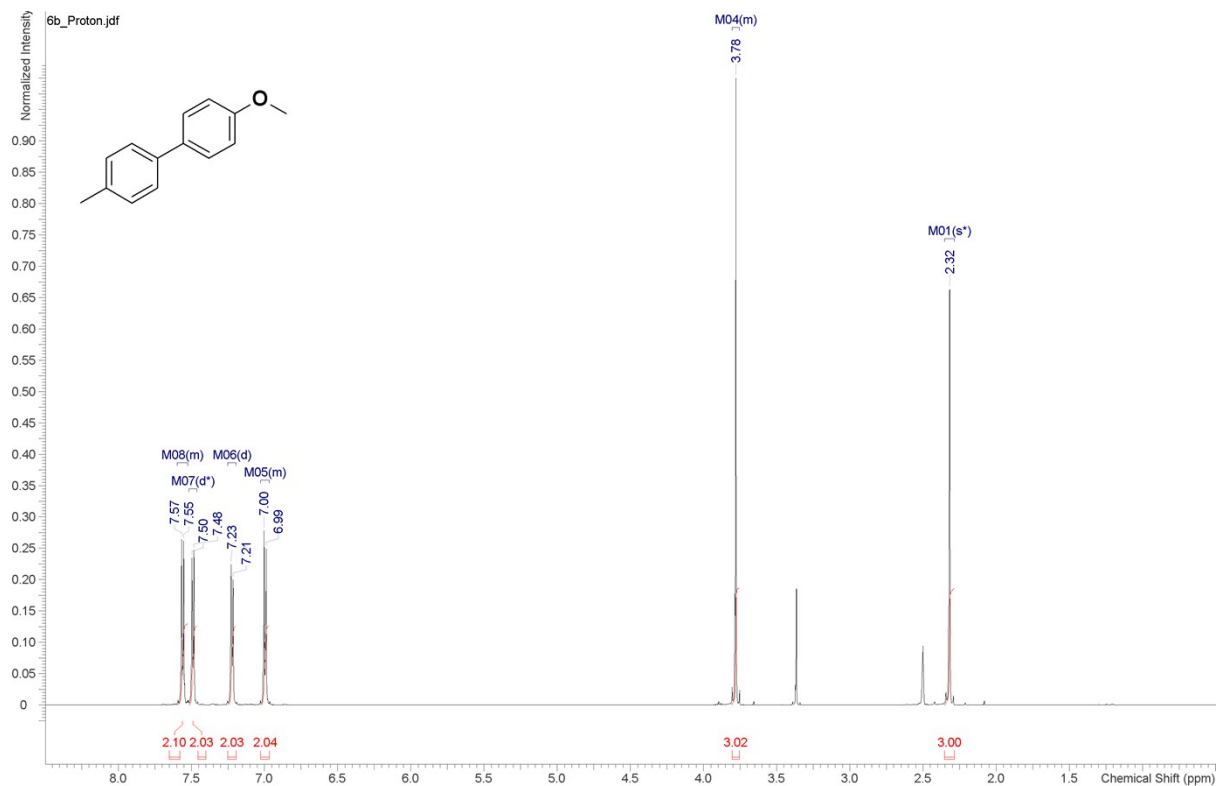


¹³C NMR

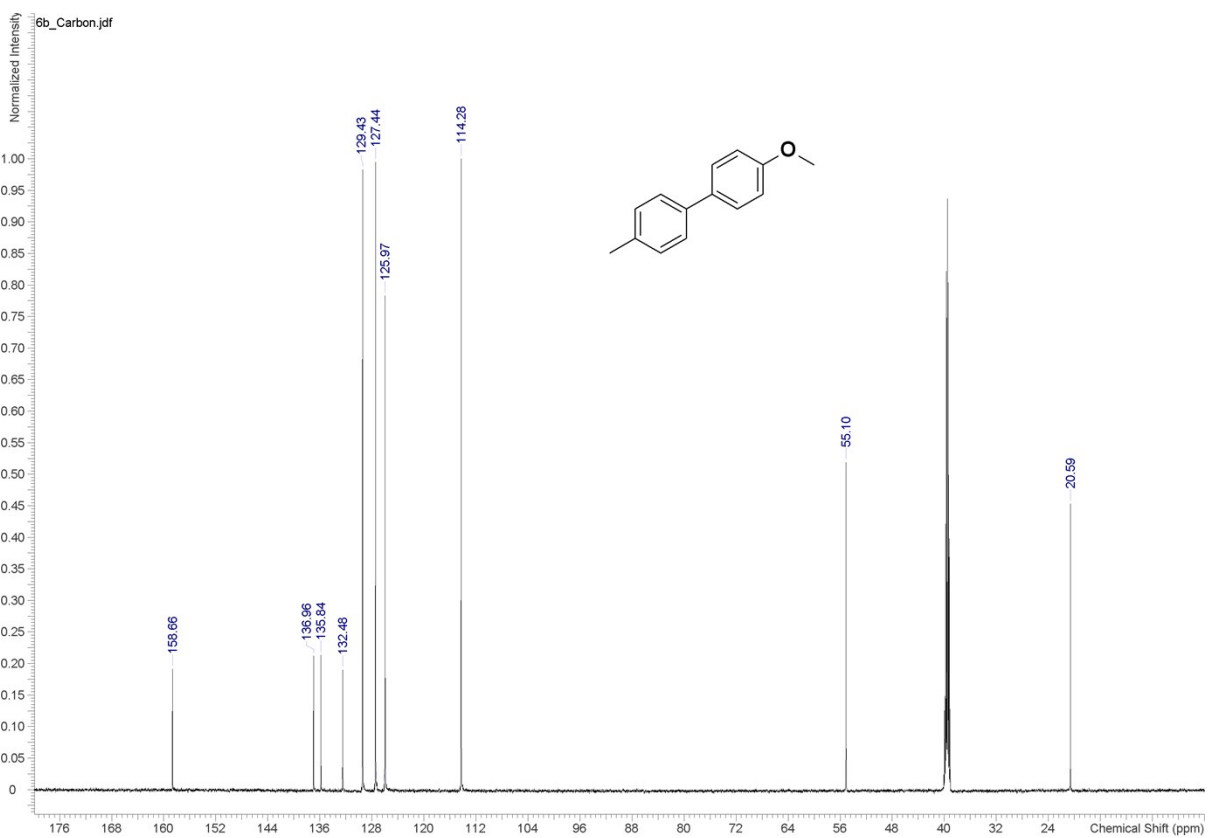


4-methoxy-4'-methylbiphenyl (6b)

¹H NMR

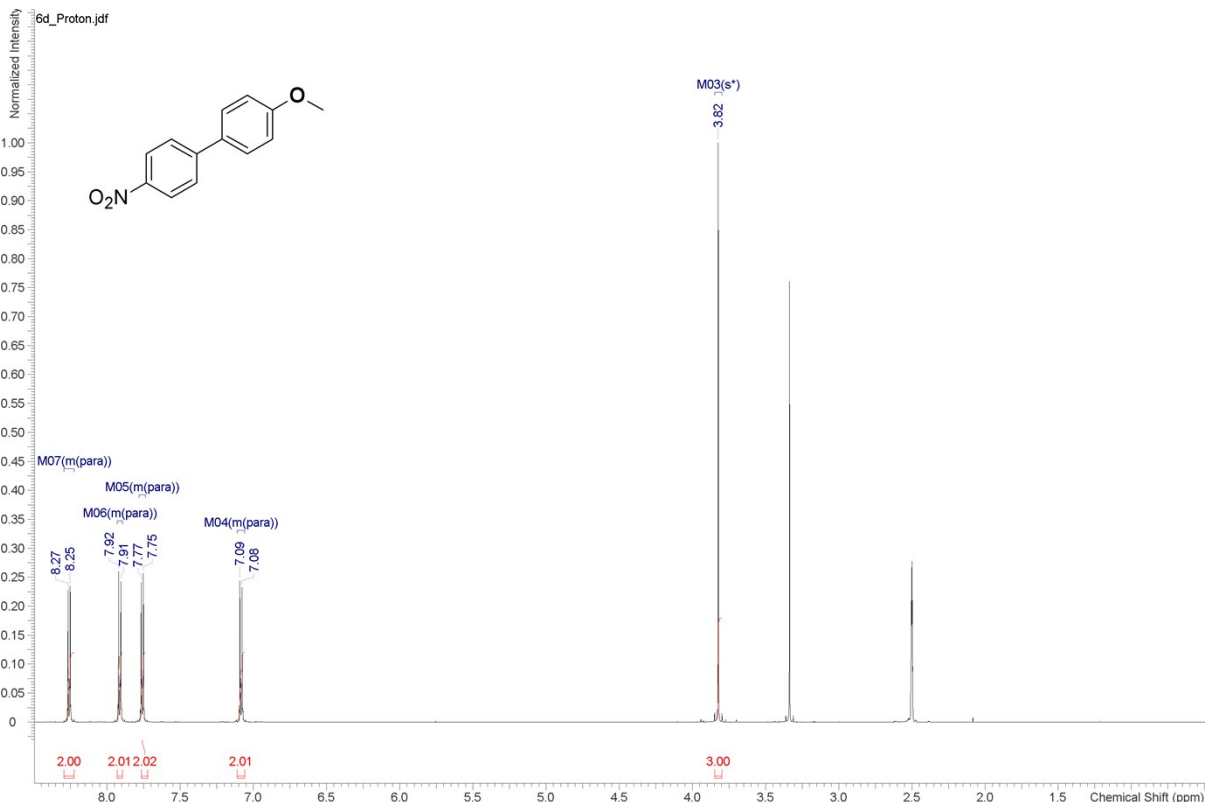


¹³C NMR

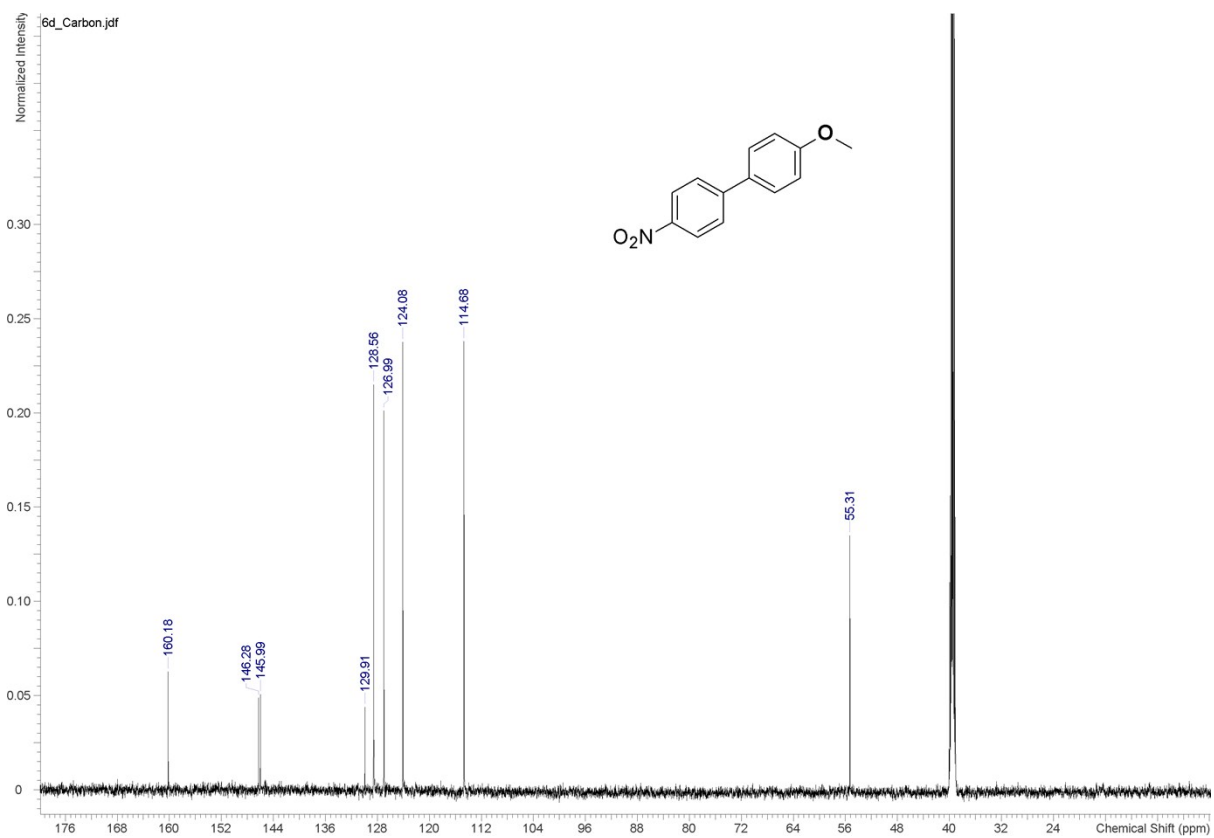


4-methoxy-4'-nitrobiphenyl (6d)

¹H NMR

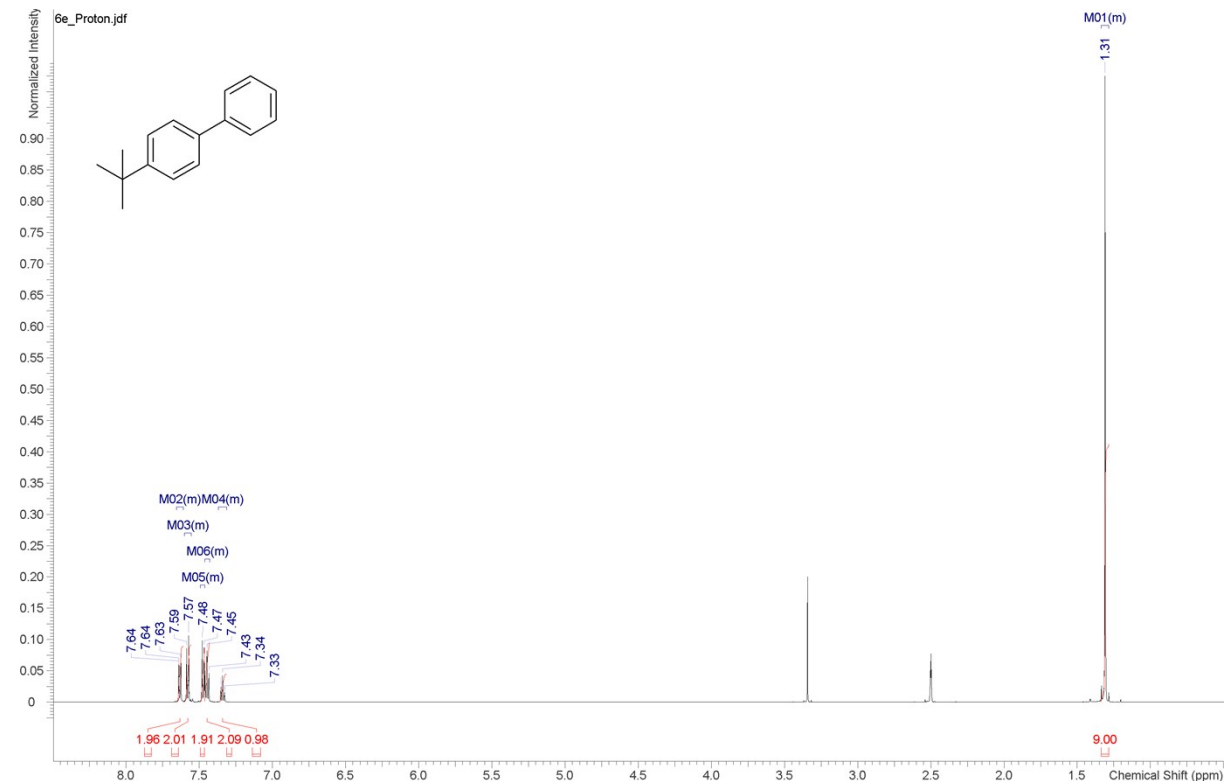


¹³C NMR

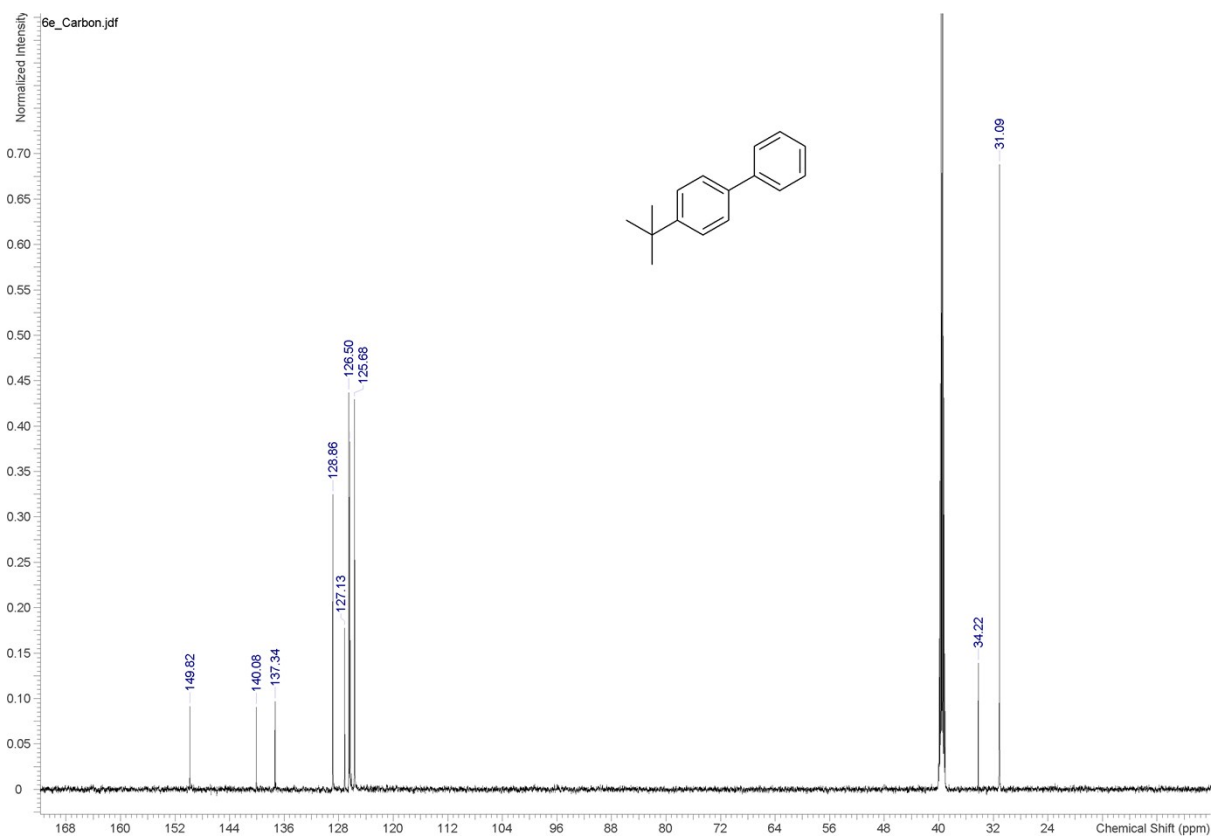


4-*tert*-butylbiphenyl (6e)

¹H NMR

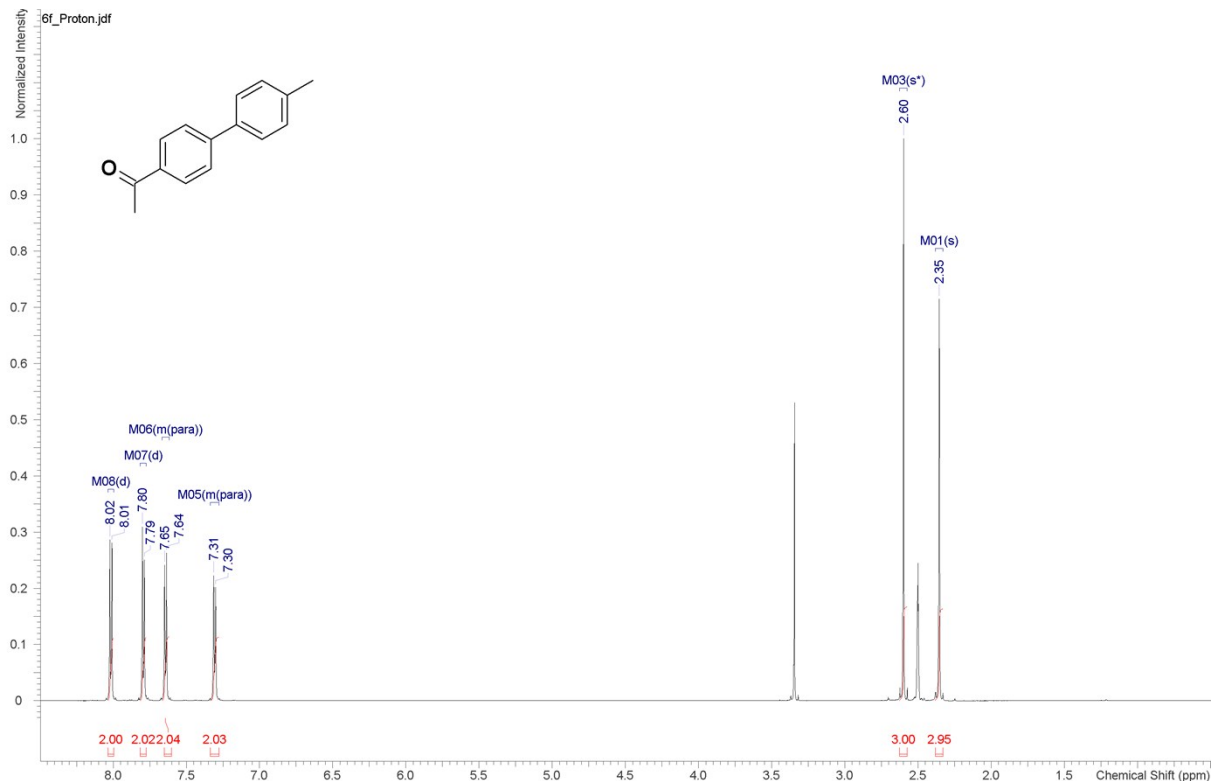


¹³C NMR

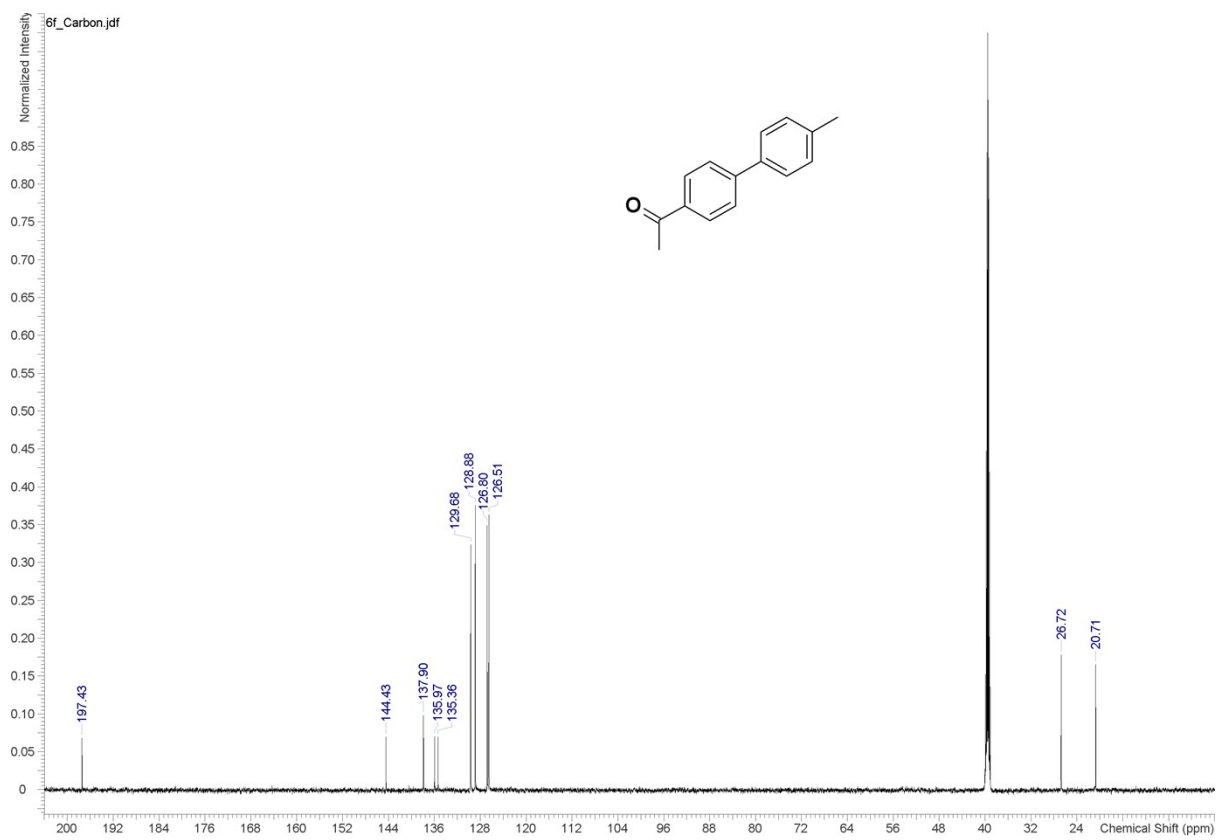


1-(4'-methylbiphenyl-4-yl)ethanone (6f)

¹H NMR

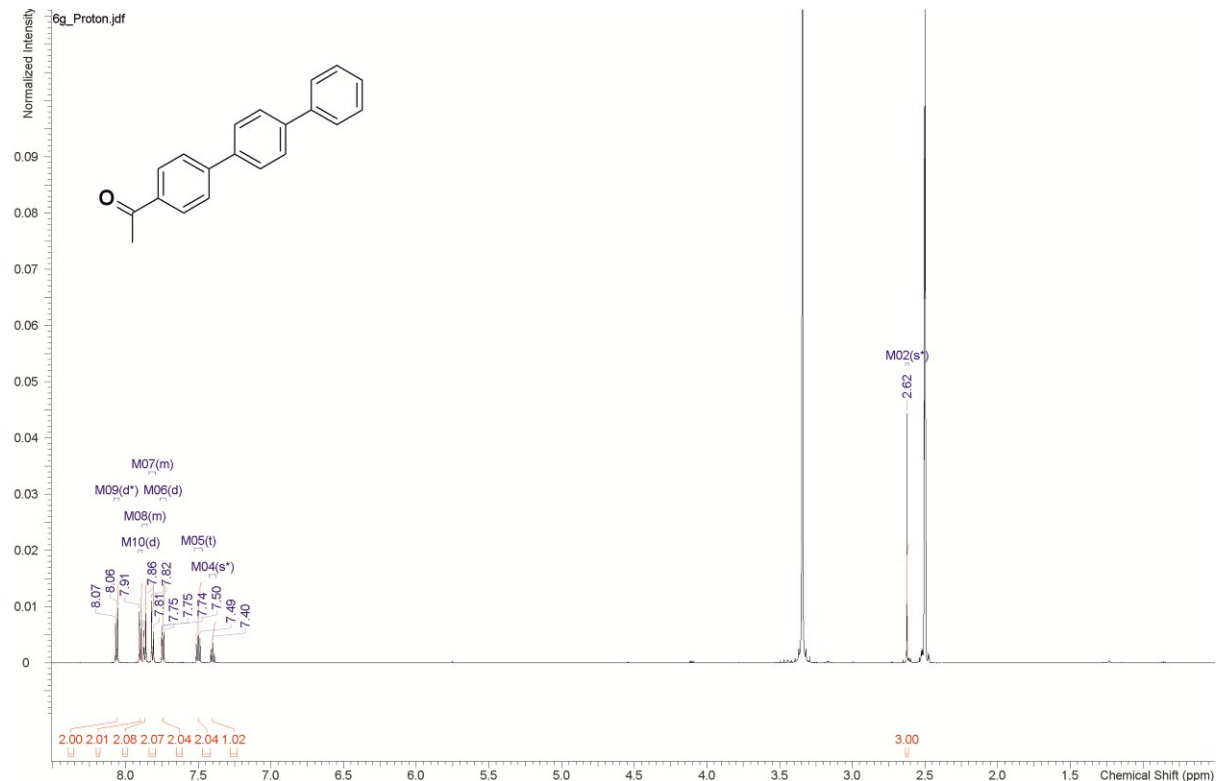


¹³C NMR

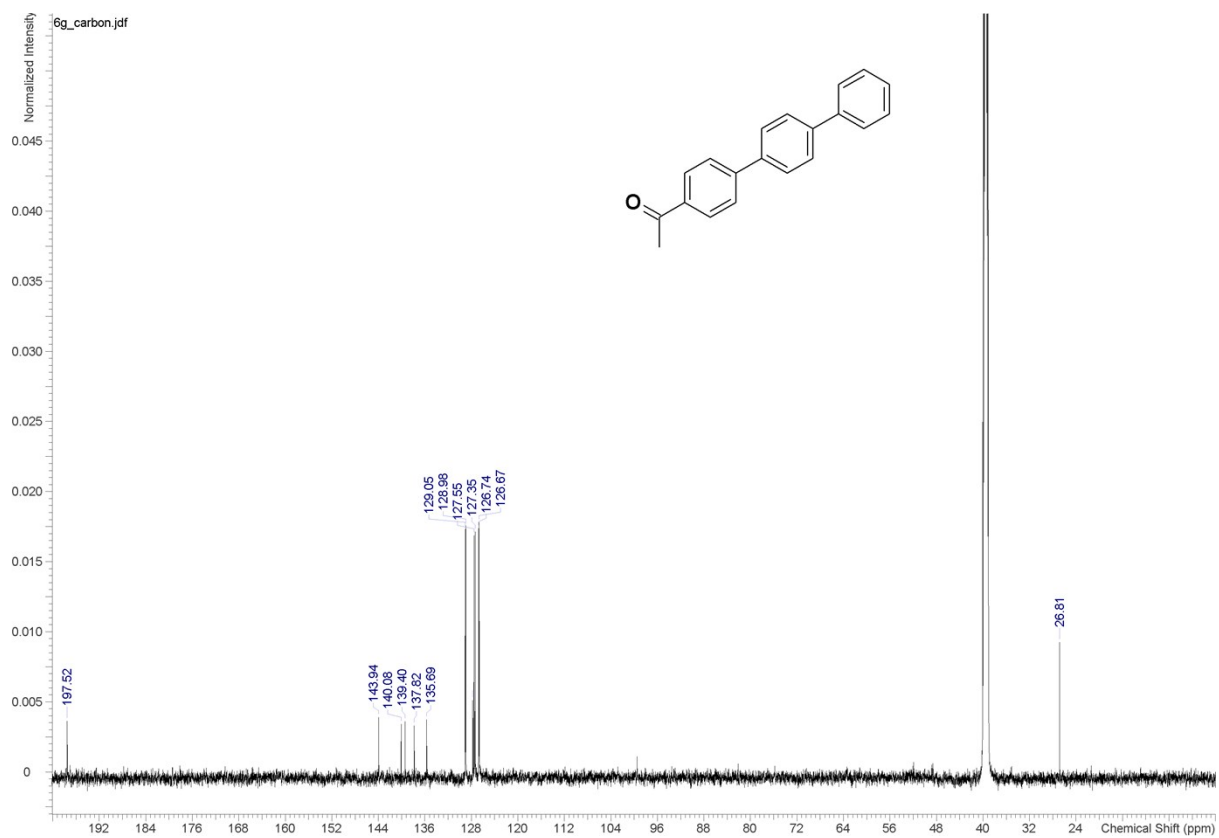


1-(1,1':4',1''-terphenyl-4-yl)ethanone (6g)

¹H NMR

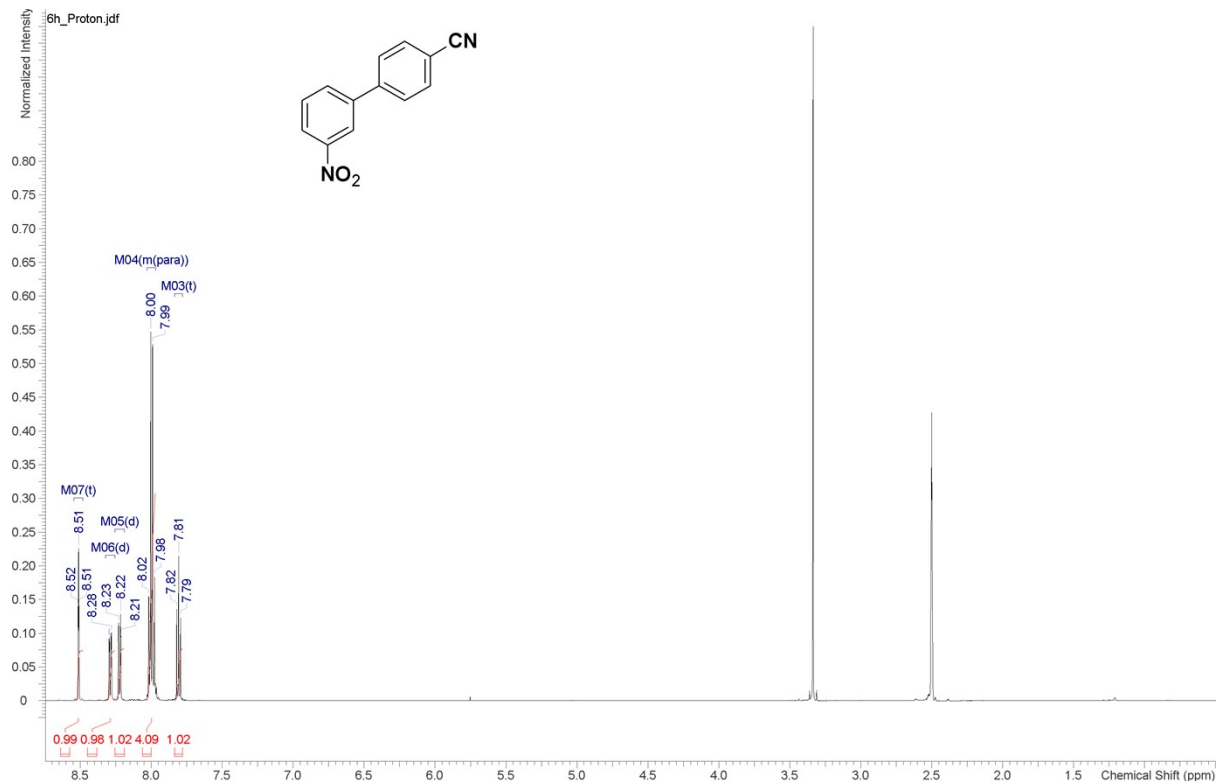


¹³C NMR

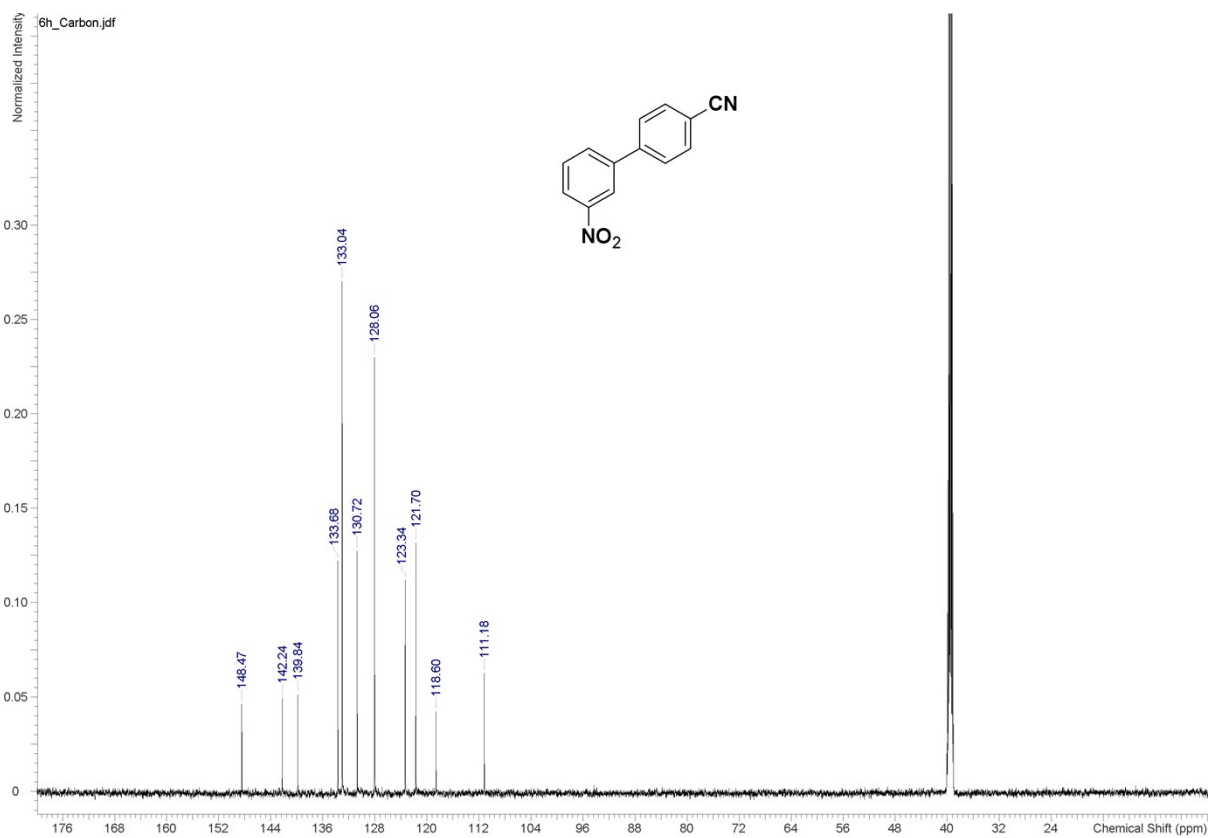


3'-nitrobiphenyl-4-carbonitrile (6h)

¹H NMR

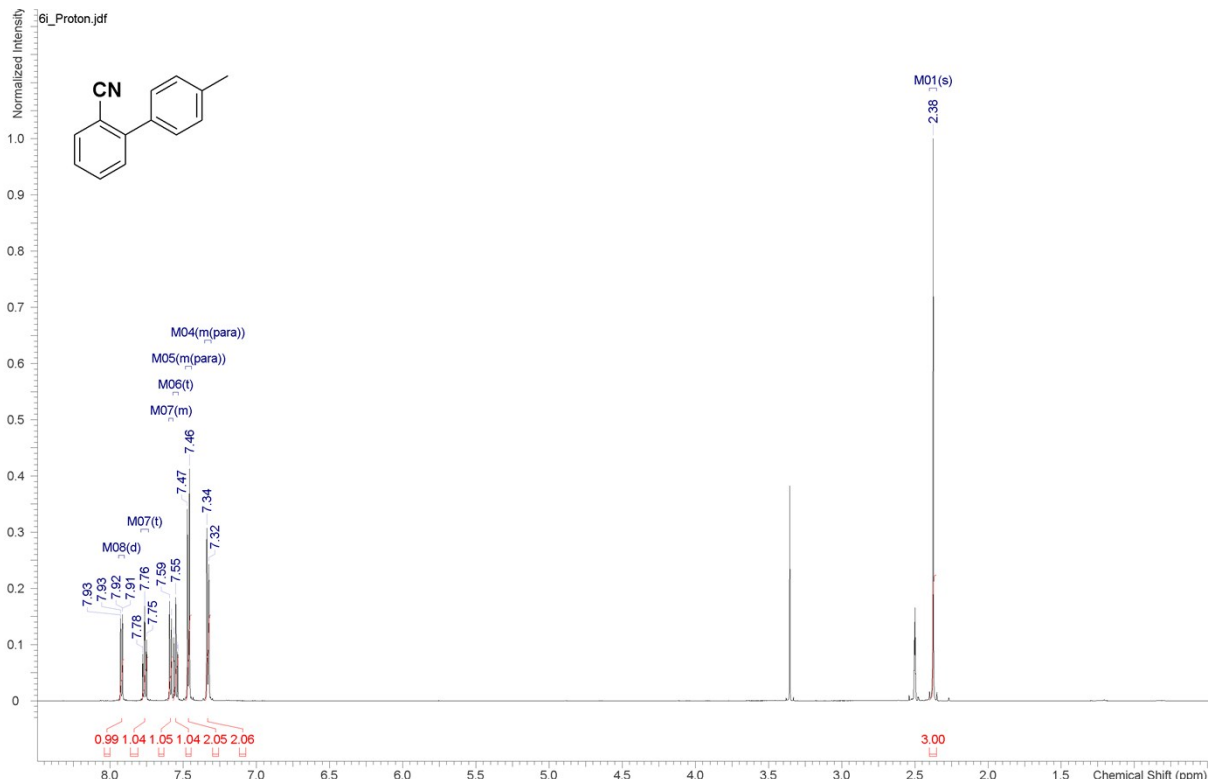


¹³C NMR

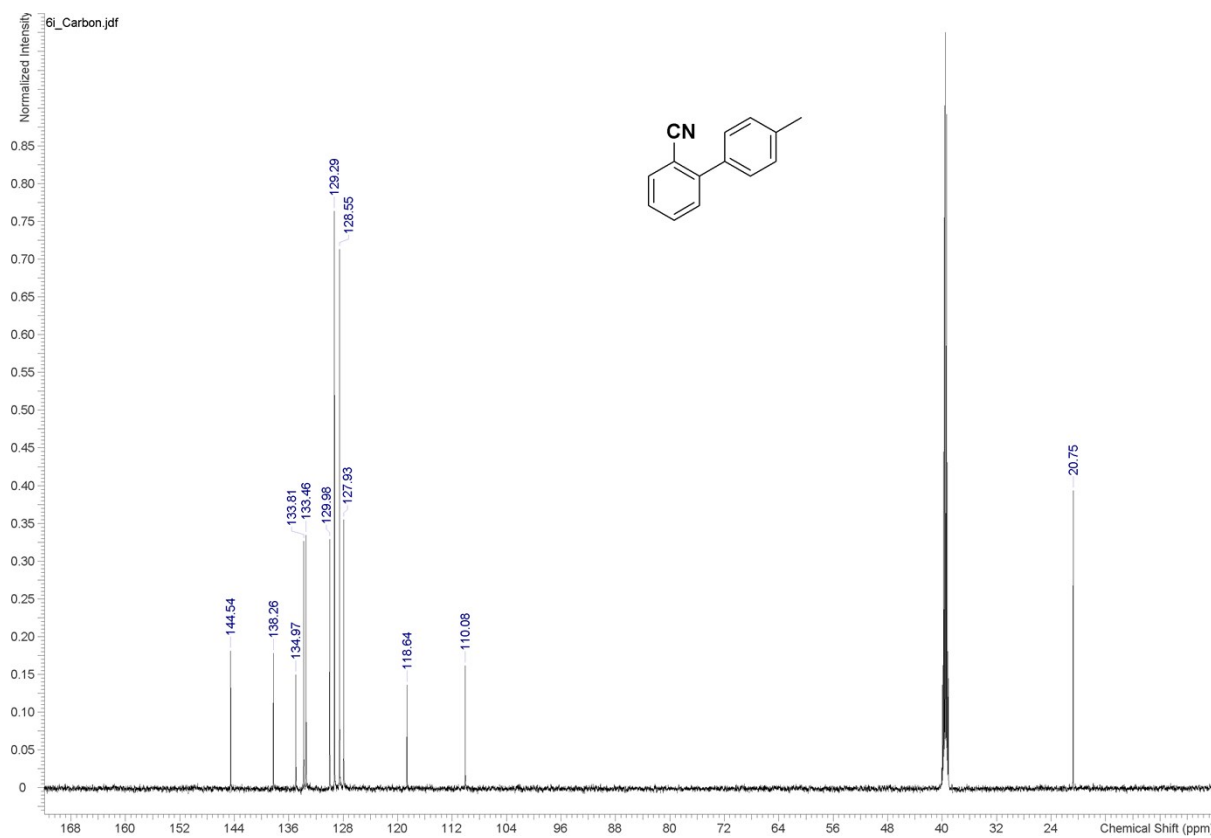


4'-methylbiphenyl-2-carbonitrile (6i)

¹H NMR



¹³C NMR



References

1. T. Tagata and M. Nishida, *J. Org. Chem.* 2003, **68**, 9412.
2. A. Cwik, Z. Hell and F. Figueras, *Org. Biomol. Chem.* 2005, **3**, 4307.
3. K. Shimizu, T. Kan-no, T. Kodama, H. Hagiwara and Y. Kitayama, *Tetrahedron Lett.*, 2002, **43**, 5653.
4. K. Mori, K. Yamaguchi, T. Hara, T. Mizugaki, K. Ebitani and K. Kaneda, *J. Am. Chem. Soc.*, 2002, **124**, 11572.
5. S. Wei, Z. Ma, P. Wang, Z. Dong and J. Ma, *J. Mol. Catal. A: Chem.*, 2013, **370**, 175.
6. H. A. Patel, A. L. Patel and A. V. Bedekar, *Appl. Organomet. Chem.* 2015, **29**, 1.
7. C. M. Crudden, M. Sateesh and R. Lewis, *J. Am. Chem. Soc.*, 2005, **127**, 10045.
8. A. Papp, G. Galbacs and R. Molnar, *Tetrahedron Lett.*, 2005, **46**, 7725.
9. S. Noel, C. Luo, C. Pinel and L. Djakovitch, *Adv. Synth. Catal.*, 2007, **349**, 1128.
10. K. Song, P. Liu, J. Wang, L. Pang, J. Chen, I. Hussain, B. Tan and T. Li, *Dalton Trans.*, 2015, **44**, 13906-13913
11. Y.Q. Zhang, X.W. Wei and R. Yu, *Catal Lett.*, 2010, **135**, 256.
12. R. Li, P. Zhang, Y. Huang, P. Zhang, H. Zhong and Q. Chen, *J. Mater. Chem.*, 2012, **22**, 22750.
13. Y. Jang, J. Chung, S. Kim, S. W. Jun, B. H. Kim, D. W. Lee, B. M. Kim and T. Hyeon, *Phys. Chem. Chem. Phys.*, 2011, **13**, 2512.
14. S. Wei, Z. Ma, P. Wang, Z. Dong and J. Ma, *J. Mol. Catal. A: Chem.* 2013, **370**, 175.
15. C. M. Crudden, M. Sateesh and R. Lewis, *J. Am. Chem. Soc.*, 2005, **127**, 10045.
16. F. Zhang, J. Jin, X. Zhong, S. Li, J. Niu, R. Li and J. Ma, *Green Chem.*, 2011, **13**, 1238.
17. A. V. Martínez, A. Leal-Duaso, José I. García, J. A. Mayoral, *RSC Adv.*, 2015, **5**, 59983.
18. A. Z. Wilczewska and I. Misztalewska, *Organometallics*, 2014, **33**, 5203.
19. C.-H. Ying, S.-B. Yan, and W.-L. Duan, *Org. Lett.*, 2014, **16**, 500.
20. Y.-Q. Yuan, and S.-R. Guo, *Synth. Commun.*, 2012, **42**, 1059.
21. X. Cui, Z. Li, C.-Z. Tao, Y. Xu, J. Li, L. Liu, and Q.-X. Guo, *Org. Lett.*, 2006, **8**, 2467.
22. Y. Peng, J. Chen, J. Ding, M. Liu, W. Gao, and H. Wu, *Synthesis*, 2011, **2**, 2136.
23. B. V. Rokade, and K. R. Prabhu, *J. Org. Chem.*, 2012, **77**, 5364.

24. T. Kawamoto, A. Sato, and I. Ryu, *Org. Lett.*, 2014, **16**, 2111.
25. X. Chen, H. Ke, and G. Zou, *ACS Catal.*, 2014, **4**, 379.
26. E. Yamamoto, K. Izumi, Y. Horita, and H. Ito, *J. Am. Chem. Soc.*, 2012, **134**, 19997.
27. C. Zhou, Q. Liu, Y. Li, R. Zhang, X. Fu, and C. Duan, *J. Org. Chem.*, 2012, **77**, 10468.
28. J. M. Antelo Miguez, L. A. Adrio, A. Sousa-Pedrares, J. M. Vila, and K. K. Hii, *J. Org. Chem.*, 2007, **72**, 7771.
29. J. M. Antelo Miguez, L. A. Adrio, A. Sousa-Pedrares, J. M. Vila, and K. K. Hii, *J. Org. Chem.*, 2007, **72**, 7771.
30. B. Tao, and D. W. Boykin, *J. Org. Chem.*, 2004, **69**, 4330.
31. G. A. Edwards, M. A. Trafford, A. E. Hamilton, A. M. Buxton, M. C. Bardeaux, and J. M. Chalker, *J. Org. Chem.*, 2014, **79**, 2094.